UNIVERSITÀ POLITECNICA DELLE MARCHE
Department of Agricultural, Food and Environmental Sciences (D3A)
PhD Course in Agricultural, Food and Environmental Sciences (XVIII cycle)

Characterization of a transcription factor controlling vitamin B3 metabolism in plant growth promoting rhizobacteria

Advisor:
Prof.ssa Nadia Raffaelli

Ph.D. Dissertation of:
Gabriele Minazzato

Academic years 2016/2017 - 2018/2019

Contents

List of Figures

List of Tables

1. INTRODUCTION

1.1 Plant Growth Promoting Rhizobacteria

Soil is an excellent niche for many microorganisms: protozoa, fungi, viruses, and bacteria. Some microorganisms are able to colonize the soil surrounding plant roots, named rhizosphere, thanks to the influence of plant roots excreted metabolites (Kennedy, 2005). Rhizosphere bacteria, in particular Rhizobacteria, are able to colonize plant roots at all stages of plant growth, in the presence of a competing microflora (Antoun and Kloepper, 2001). Within this group, plant growth promoting rhizobacteria (PGPR) are able to establish a beneficial interaction with roots plant, enhancing the hosts growth and development with no external sign of infection, or detectable negative effects on the plant host (Kloepper, 2003).

In the rhizosphere, the composition and the amount of exudates coming from roots plant are largely affected by multiple factors such as plant species and age, root region, pH, temperature and surrounding microbes (Rovira 1969). Half of photosynthetically fixed C by plant is released into external environment in rhizosphere as root exudates, with organic acids (citrate, malate, succinate, pyruvate, fumarate, oxalate, and acetate) and sugars (glucose, xylose, fructose, maltose, sucrose, galactose, and ribose) representing the major fraction, and variable amounts of α-aminoacids, nucleobases, vitamins, fatty acids and enzymes (Rovira, 1969). PGPRs use these nutrients present in the root plant exudates for their development. In turn, bacteria produce other molecules and enzymes that are responsible of the regulation of plant's hormonal level, nutrient resource acquisition, and biocontrol of different pathogens. Root exudates promote a selection of specific groups of bacteria in the rhizosphere, among which are PGPRs, which are completely different to the microbial population present in free-soil.

PGPRs can be classified into extracellular plant growth promoting rhizobacteria (ePGPRs) and intracellular plant growth promoting rhizobacteria (iPGPRs) (Martinez-Viveros *et al.,* 2010). The ePGPRs can be found free in the rhizosphere, while iPGPRs are generally located inside specialized nodular structures of roots. Nodules are specialized root cells originated from the root symbiosis with the intracellular bacteria. After the invasion of bacteria on the surface of hair roots, the plant creates a spherical

structure in the infected area where bacteria fit and grow. Usually this structure is specific of bacteria that exhibit nitrogen fixation, such as Rhizobia (Cocking, 2003).

The bacterial genera *Agrobacterium, Arthrobacter, Azotobacter, Azospirillum, Bacillus, Burkholderia, Caulobacter, Chromobacterium, Erwinia, Flavobacterium, Micrococcous, Pseudomonas and Serratia* belong to ePGPRs (Ahemad *et al.,* 2014), while iPGPRs comprise the family of Rhizobiaceae and include *Allorhizobium*, *Bradyrhizobium*, *Mesorhizobium* and *Rhizobium* (Bhattacharyya *et al.,* 2012).

PGPRs are able to stimulate plant growth either directly or indirectly. Direct mechanisms usually involve the release by the microorganisms of plant growth regulators, which positively affect the metabolism of the plants, or substances which are usually in short supply (Govindasamy *et al.,* 2010). The most important direct mechanisms of plant growth stimulation by PGPRs include nitrogen fixation, phosphate and potassium solubilization, and phytohormone production (Goswami *et al.,* 2016). Indirect mechanisms involve the ability of PGPRs to eliminate harmful effects of pathogenic organisms or to protect the plant against harmful environmental conditions (abiotic stress) (Solano *et al.,* 2008). Among indirect mechanisms, the most representative are chitinase and glucanase production, antibiotic production, induction of systemic resistance (Goswami *et al.,* 2016; Solano *et al.,* 2008).

In recent years, the interest in the use of PGPRs in agriculture to promote plant growth has increased. In agreement with Dardanelli *et al.,* (2010), the presence of microorganisms in the soil is fundamental to the maintenance of soil function, in both natural and managed agricultural soils. Microbes are involved in key processes such as soil structure formation, decomposition of organic matter, toxin removal, and cycling of elements (carbon, nitrogen, phosphorus, potassium, and sulfur). It is clear that beneficial soil microorganisms represent agricultural inputs for improving crop production. In this view, different beneficial properties of PGPRs (Table 1) can be exploited for the development of a sustainable agriculture. These bacteria respect the common free-soil living bacteria, can be used effectively in nutrient-deficient soils, favoring the reduction of chemical fertilizers and supporting environment-friendly crop productivity (Requena *et al.,* 1997). In addition, PGPRs have great adaptation to difficult environments including drought stress (Arzanesh *et al.,* 2011), salt stress (Mayak *et al.,* 2004), high temperatures, dryness or heavy rainfalls in tropical countries, and contaminated environments (Burd *et*

al., 2000; Dell'Amico *et al.,* 2008), indicating that they could contribute to improve plant crops cultivation in areas not suitable for agriculture.

Genus	Species	Plant Host	Effects on Plant	Reference
Acinetobacter	*baylyi*	Wheat	Improvement of plant growth and nutrition under salt stress	Huddedar S.B. et al. (2002); Appl. Bioche. 102: p.21.
Agrobacterium	*tumefaciens*	Lettuce	Enhancement of root elongation by phytohormones	Barazani O. Z et al. (1999); Journal of Chemical Ecology, 25(10): p.2397.
Arthrobacter	*chlorophenolicus*	Bean	Enhancement of phytoremediation	Scheublin T. R. et al. (2014); Environmental Microbiology 16(7): p.2212.
Azotobacter	*vinelandii*	Tomato	Improvement of plant growth by phytohormones	Azcorn R. et al. (1975); Plant Soil. 43: p.609.
Bacillus	*subtilis*	Higher plants	Enhancement of shoot and root growth	Sivasakthi S. et al. (2014); African journal of agri rsch. 9(16): p.1265.
Bradyrhizobium	*sp. BTAi1*	Rice	Improvement of plant growth by nitrogen fixation	Chaintreuil C. et al. (2000); Appl. Environ. Microbiol. 66(12): p.5437
Burkholderia	*phytofirmans strain PsJN*	Potato	Enhancement of plant vigor and resistance to stresses	Weilharter A. et al. (2011); Journal of Bacteriology 193(13): p.3383.
Enterobacter	*hormaechei ATCC 49162*	Wheat	Phosphate solubilization and IAA production	Walpola B. C. et al. (2015); Tropical Agricultural Research & Extension 18(1).
Klebsiella	*spp.*	Rice	Improvement of plant growth by phytohormones	El-Khawas H. et. al. (1999); Biology and Fertility of Soils 28(4): p.377.
Mesorhizobium	*spp.*	Chickpea	Promotion of Nodulation and nitrogen fixation	Verma J. et al. (2013); Ecological Engineering 51: p.282.
Methylobacterium	*sp. PPFM-Ah*	Groundnut	Induction of pathogen plant stress resistance	Madhaiyan M. et al. (2006); Current microbiology 53(4): p.270
Nitrobacter	*spp.*	Tomate	Phosphate solubilization and IAA production	Ibiene A. et al. (2012); Journal of American Science 8(2): p.318.
Pseudomonas	*fluorescens Pf-5*	Cocumber	Induction of pathogen plant stress resistance	Kraus J. et al. (1992); Phytopathology 82(3): p.264.
Rhizobium	*leguminosarum*	Pea	Promotion of Nodulation and nitrogen fixation	Ma W. et al. (2003); Appl. Environ. Microbiol. 69: p. 4396.
Rhodopseudomonas	*palustris*	Rice	Enhancement of plant vigor and resistance to salt stresses	Kantha T. et al. (2015); Annals of microbiology 65(4): p. 2109.
Serratia	*marcescens*	Bean	Induction of pathogen plant stress resistance	Ordentlich A. et al. (1987); SoilBiol. Biochem. 19: p. 747.
Sinorhizobium	*meliloti*	Lettuce	Enhancement of shoot and root biomass	Galleguillos C. et al. (2000); Plant Science 159(1): p. 57.

Table 1: PGPRs genera whose genome has been fully sequenced and whose beneficial interactions with the host plant have been experimentally demonstrated.

1.2 Involvement of vitamins of the B group in PGPRs colonization and plant growth

Plants under perfect growth conditions usually synthesize adequate amount of most vitamins. However, abiotic stresses (such as drought, temperature fluctuations, and mineral deficiency) often cause vitamin deficiency, resulting in loss of plant fitness.

Vitamins are essential for the plants metabolism, and they are known to increase the production of essential compounds (Asensi-Fabado and Munné-Bosch 2010; Smith *et al.,* 2007), neutralize the negative consequences of the lack of adequate minerals, induce biological resistance against pathogens (Paré *et al.,* 2005; Kloepper and Ryu 2006). Under natural conditions, vitamins administration increases plant growth and yield (Derylo and Skorupska 1993).

Some plant species cannot synthetize all the required vitamins, but the exudate of these plants can be a source of vitamin precursors that are converted into vitamin by bacteria. Once produced, vitamins are absorbed by the host plant. In fact, plant roots are able to absorb vitamins from exogenous sources, with positive impacts on root extension, stem length, dry matter production and nutrients absorption. Among plant species that cannot self-produce all the required vitamins are alfalfa, soybean, pea, bean, red clover, and *Pleurochrysis carterae* (Shaukat-Ahmed 1961; Marek-Kozaczuk and Skorupska 2001; Miyamoto *et al.,* 2002). These plants tend to overcome this deficiency by maintaining interaction with PGPRs in the rhizosphere. In this way, they take advantage of the bacterial capacity to produce vitamins.

It is well reported that seven vitamins of the B group are produced in significant quantities by PGPRs. They are biotin (vitamin B7), cobalamin (vitamin B12), niacin (vitamin B3), pantothenic acid (vitamin B5), pyridoxine (vitamin B6), riboflavin (vitamin B2) and thiamine (vitamin B1). As an example, *Azotobacter vinelandii* strain ATCC 12837 and *A. chroococcum* strain H23, PGPR species that contribute to N_2-fixation, have been shown to produce niacin, pantothenic acid, thiamine, riboflavin, and biotin after 72 h of growth in chemically defined media (Revillas *et al.,* 2000). However, the role of the PGPRs production of vitamins, with particular regards to the B-group, on plant growth and health has been poorly investigated compared to their role in bacterial metabolism (Palacios *et al.,* 2014).

In 1993 Derylo and Skorupska analyzed plant growth and symbiotic N_2-fixation in red clover after inoculation with *Rhizobium* or co-inoculation with *Rhizobium* and *Pseudomonas fluorescens* strain 267. The interaction between the two microorganisms and the plant resulted in a significant increase of shoot and nodule weights in comparison with the control plants inoculated with *Rhizobium* only. Authors observed that, in presence of the vitamin-producing *P. fluorescens* or in growth medium supplemented with vitamins, the red clover showed higher nitrogenase activity and higher fresh and dry weight. This suggests that *Rhizobium*-clover plant symbiosis was limited by the lack of

vitamins. However, the vitamin responsible for the increase in N_2-fixation was not identified.

In 2001 Marek-Kozaczuk and Skorupska confirmed that clover growth promotion in gnotobiotic conditions was caused by an increase in *Rhizobium* N_2-fixation, supported by vitamin B released by the *P. fluorescence* strain 267. Authors established that such strain produced thiamine, niacin, biotin, pantothenic acid, pyridoxine and cobalamine, and hypothesized that the vitamin production by the *P. fluorescence* strain may supplement the nutritional requirement of Rhizobia, finally resulting in improvement of plant growth.

Indole-3-acetic acid (IAA) is the most common phytohormone in plants (Zhao, 2010). The most important effect of IAA is to promote development of roots and stems, through stretching of the newly formed cells in the meristem and promotion of their division (Guilfoyle and Hagen, 2007). Zakharova *et al.,* (2000) have demonstrated that *Azospirillum brasilense* promotes IAA synthesis under the influence of six water-soluble vitamins (pyridoxine, riboflavin, thiamine, biotin, nicotinic acid and nicotinamide). Authors showed that the addition of different concentrations of these vitamins (10-100µg/l) in the bacterium culture medium resulted in the synthesis of IAA in a vitamin dose-dependent manner. The best enhancers of IAA synthesis were pyridoxine and nicotinic acid. The idea was that the effect of nicotinic acid was related to the implication of this vitamin as the precursor of NAD, which is used as coenzyme in the IAA biosynthetic pathway.

Based on these examples, the presence of an adequate amount of B-group vitamins in rhizosphere can be considered one of the factors that affect the microbial capacity for root colonization and plant growth promotion (Rovira and Harris 1961; Streit *et al.,* 1996).

1.3 Overview of Vitamin B3 biosynthesis in bacteria

Vitamin B3 (also known as niacin or vitamin PP) comprises nicotinic acid (Na), nicotinamide (Nam) and nicotinamide riboside (Nr). These molecules are all precursors of Nicotinamide adenine dinucleotide (NAD), which is the biologically active form of the vitamin.

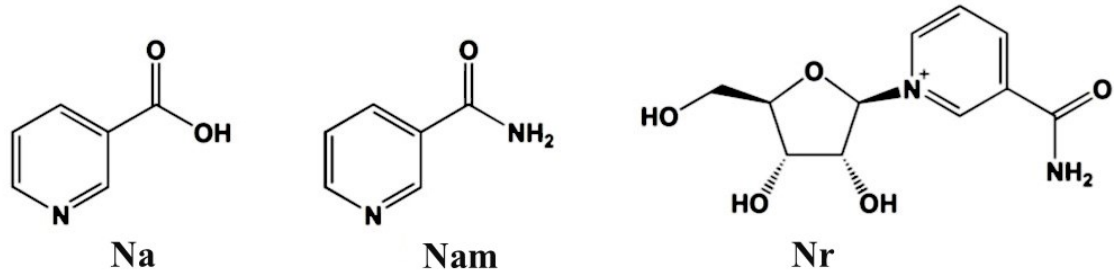

Figure 1: Structures of the three principal forms of vitamin B3: Na: nicotinic acid; Nam: nicotinamide; Nr: nicotinamide riboside.

NAD is an important redox coenzyme of several dehydrogenases due to its ability to assume two metabolic forms: the oxidized and the reduced one. NAD is also used in many metabolic and regulatory processes as a consumable co-substrate and therefore, its continuous resynthesis is essential for living cells (Gazzaniga *et al.,* 2009).

A peculiar feature of the biosynthetic pathway of vitamin B3 is that cells first synthetize NAD starting from simple precursors (amino acids and sugar) and once formed NAD itself becomes the source of vitamin B3. In many prokaryotes, the *de novo* synthesis of NAD (Figure 2A) starts from the amino acid aspartate and the intermediate of glycolysis dihydroxyacetone-phosphate (DHAP). These metabolites are converted to quinolinate (QA) via the enzymatic activities of L-aspartate oxidase -NadB- and QA synthase -NadA-. Then QA is processed by a QA-phosphoribosyl transferase -NadC- to yield nicotinic acid mononucleotide (NaMN), in a reaction requiring phosphoribosyl pyrophosphate (PRPP). NaMN is finally converted into NAD via a nicotinic acid mononucleotide (NaAD) intermediate, by a two-step conversion catalyzed firstly by nicotinate-nucleotide adenylyltransferase -NadD- and then by NAD-synthetase -NadE- (Gazzaniga *et al.,* 2009). However there are bacteria such as *Haemophilus influenzae*, which do not carry genes for a *de novo* pathway (Fleischmann *et al.,* 1995), and bacteria such as *Cytophaga hutchinsonii*, which carry the genes for a *de novo* pathway from the amino acid tryptophan (Kurnasov *et al.,* 2003), a route that mainly occurs in eukaryotes.

As described above, the intracellular catabolism of NAD generates the three forms of vitamin B3 that can be recycled back to the coenzyme through distinct salvage pathways. Na, Nam and Nr can also be released in the extracellular environment and used as exogenous NAD precursors by other cells. A brief description of the different salvage pathways is given below:

Na is converted to NaMN by Nicotinate phosphoribosyltransferase -PncB-. The produced NaMN then enters the *de novo* pathway (Figure 2B).

NaM is transformed to Na by nicotinamidase - PncA- and conversion to NAD follows the same route described for Na (Figure 2C). Alternatively, Nam can be converted directly to nicotinamide mononucleotide (NMN) by the enzyme nicotinamide-phosphoribosyltransferase -NadV-. Then, the enzyme Nicotinamide-mononucleotide adenylyltransferase -NadM- converts NMN to NAD (Figure 2C).

Nr is phosphorylated to NMN by the enzyme nicotinamide riboside kinase -NadR- and NMN is then converted to NAD by NadM. Alternatively, NMN deamidase -PncC- converts NMN to NaMN that enters the *de novo* route (Figure 2D).

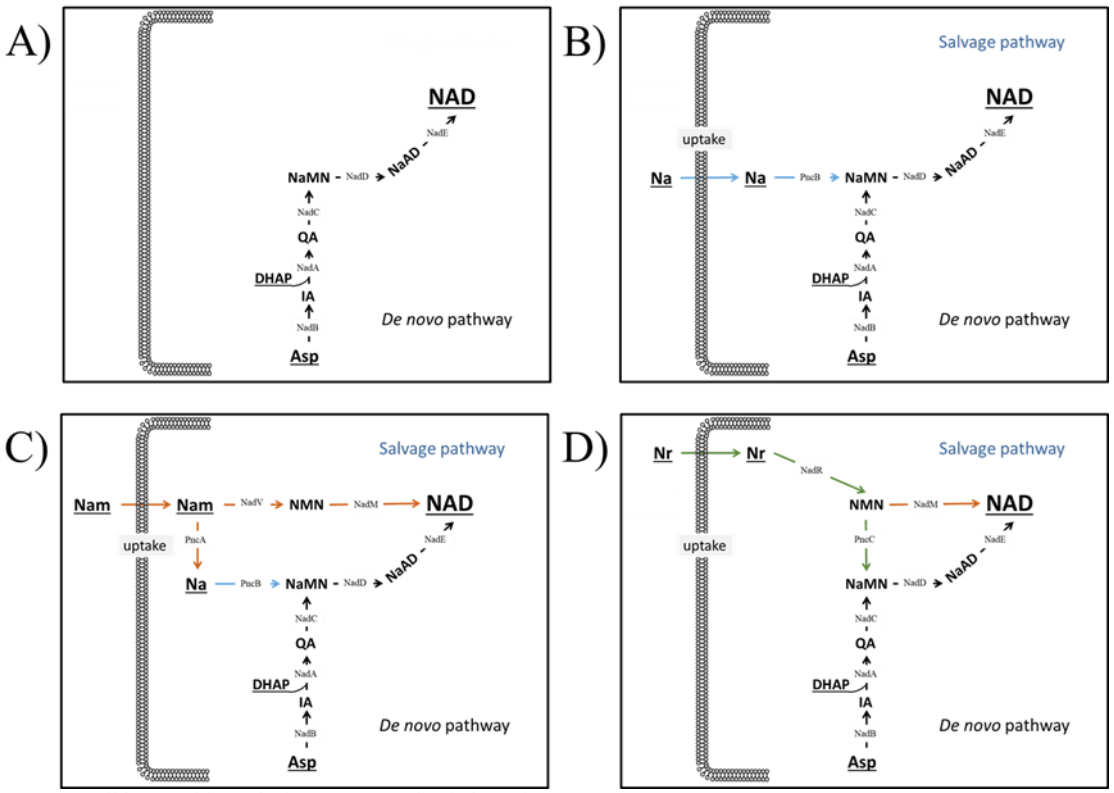

Figure 2: Possible NAD biosynthetic routes occurring in bacteria.
Abbreviations: NAD: nicotinamide adenine dinucleotide; Nr: ribosyl nicotinammide; Nam: nicotinamide; NMN: nicotinamide mononucleotide; Na: nicotinic acid; NaMN: nicotinic acid mononucleotide; NaAD: nicotinate adenine dinucleotide; DHAP: dihydroxyacetone-phosphate; QA: quinolinic acid; IA: iminoaspartate; Asp: L-aspartic acid. NadB: L-aspartate oxidase; NadA: QA-synthase; NadC: QA-phosphoribosyltransferase; NadD: Nicotinate-nucleotide adenylyltransferase; NadE: NAD-synthetase; PncB: Nicotinate phosphoribosyltransferase; PncA: nicotinamidase; NadV: nicotinamide-phosphoribosyltransferase; NadM: Nicotinamide-mononucleotide adenylyltransferase; NadR: nicotinamide riboside kinase; PncC: NMN deamidase.

Depending on the bacterial species, different combinations of the biosynthetic routes described above can be operative (Sorci *et al.,* 2010). Bacteria typically prioritize the use of salvage pathways over *de novo* NAD biosynthesis (Penfound and Foster, 1996). On the other hand, the absence of endogenous and exogenous NAD precursors that contain a pyridine ring forces bacteria to synthesize NAD *de novo* (Brenner *et al.,* 2005).

The modulation in the use of the two pathways is permitted by fine regulation of the different routes performed by transcription factors, proteins that possess a specific domain to bind the promoter regions of the genes that should be regulated.

1.4 Evidence of Vitamin B3 involvement in PGPRs colonization and plant growth

NAD and all its pyridine nucleotides derivatives play a key role in many plants defense mechanisms and signaling reactions, such as production of nitric oxide and metabolism of reactive lipid derivatives (Crawford and Guo, 2005; Mano *et al.,* 2005). They are also involved in the signaling of the oxidative stress through reactive oxygen species (ROS) since they are crucial in the regulation of both ROS-producing and ROS-consuming systems (Møller, 2001; Apel and Hirt, 2004). In addition, studies have shown that Na, Nam, QA, NaAD, and NAD are all sources of the pyridine ring for the synthesis of defensive pyridine alkaloids (Ashihara *et al.,* 2015) such as nicotine and ricinine (Frost *et al.,* 1967; Waller *et al.,* 1966).

Moreover, the role of NAD and its related compounds in response to pathogen infections has also been investigated (Noctor *et al.,* 2006; Mahalingam *et al.,* 2007; Hashida *et al.,* 2009; Pétriacq *et al.,* 2012). In particular, it has been shown that in *Arabidopsis thaliana* the defense gene expression and resistance to multiple bacterial and fungal pathogens increase in presence of high level of QA, which boosts the production of NAD (Pétriacq *et al.,* 2016). In addition, treatment of *A. thaliana* with exogenous NAD induces an accumulation of salicylic acid that via the Ca^{2+}-dependent signaling pathway promotes the expression of the genes related to pathogenesis resistance to *Pseudomonas syringae* pv. Maculicola (Zhang and Mou, 2009).

In 2018, Miwa *et al.,* showed that pretreatment of *Arabidopsis* leaves and flowers, and of barley spikes with NMN enhances disease resistance versus *Fusarium graminearum*. The effect is due to the NMN induced activation of the salicylic acid-mediated signaling pathway.

In *Citrus sinensis* it was observed that exogenous NAD triggers immune responses (Alferez *et al.,* 2018), inducing a strong resistance versus citrus canker, a serious leaf and fruit disease damaging several economically important cultivars (Graham *et al.,* 2004).

All together, these studies indicate that NAD biosynthesis is involved in disease resistance against a broad range of phytopathogens in plants. In this view, the production of NAD precursors by PGPRs might boost NAD biosynthesis in plants with all the positive consequences. There are only few papers describing a role of the vitamin B3 produced by PGPRs in the promotion of plant growth.

In 2001, Marek-Kozaczuk and Skorupska showed that niacin promotes root colonization and nodulation of red clover by *Rhizobium leguminosarum bv. Trifolii*. In the first instance, Authors produced a *P. fluorescence* strain 267 mutant that was niacin auxotroph (Marek-Kozaczuk *et al.,* 2005). This mutant was inoculated on clover grown in a medium without vitamins, to study the colonization and distribution of the bacteria on the surface of roots. The level of colonization by the niacin auxotroph was ten-fold lower in comparison to the wild-type strain, which indicates that niacin is required for the successful root colonization. Subsequently, the niacin auxotroph mutant was co-inoculated with *R. leguminosarum bv. trifolii 24.1* on clover resulting in a decrease in all symbiotic parameters in comparison to coinfection with the wild type strain 267. In conclusion, the secretion of B3 vitamin by rhizosphere bacterium *P. fluorescens* strain 267 affects the colonization of clover roots.

A direct role of NAD biosynthesis in plant growth promotion by PGPRs has been demonstrated by Wang *et al.,* in 2006. Authors analyzed the beneficial interaction between potato and *Burkolderia sp.* strain PsJN. They showed that the bacterial enzyme quinolinate phosphoribosyl-transferase -NadC- was responsible of the potato growth promotion. This enzyme catalyzes the formation of nicotinate mononucleotide (NaMN) starting from quinolinate (QA), a key step in the *de novo* NAD biosynthetic pathway from aspartate (Figure 2A). The knocking out of the gene coding for NadC impairs the ability of the *Burkholderia* strain to promote the growth of potato. To verify that *nadC* was really the gene involved in plant growth promotion, the authors performed a complementation test by transforming the knockout strains with a plasmid containing a wild type *nadC* gene that fully restored the ability of growth promotion (Wang *et al.,* 2006).

1.5 Regulation of bacterial vitamin B3 biosynthesis

In general, regulation of gene expression is an important mechanism for fast adaptation of metabolism to changes in environmental conditions. Transcription factors (TF) are proteins which activate or repress gene transcription via binding to specific DNA sequences in regulatory gene regions. The binding ability of many TFs depends on the presence or absence of an effector, such as an intracellular metabolite. Currently, four different TFs are known to regulate vitamin B3 biosynthesis in bacteria. They are named NadR, NiaR, NrtR and NadQ.

1.5.1 NadR

NadR operates as a transcriptional repressor for the genes involved in the *de novo* NAD biosynthesis and in the salvage pathways starting from Nr and Na (Penfound *et al.,* 1999; Grose *et al.,* 2005). NadR occurrence is restricted to a compact phylogenetic group of Enterobacteria, such as *E. coli* and *Salmonella* (Rodionov, 2007). A dimeric form of NadR specifically binds to a palindromic 18-bp DNA sequence with consensus TGTTTA-N6-TAAACA upstream of the promoter region of the regulated genes (Penfound *et al.,* 1999, Gerasimova and Gelfand, 2005). NadR is a trifunctional protein, because in addition to its role as transcriptional repressor mediated by the N-terminal helix-turn-helix (HTH) DNA-binding domain (Aravind *et al.,* 2005), it also possess two enzymatic activities, a NMM adenylyltransferase (NadM) and an Nr kinase (NRK) activity, encoded in its central domain and C-terminal domain, respectively (Raffaelli *et al.,* 1999; Kurnasov *et al.,* 2002).

The central domain of NadR operates also as an effector domain that modulates the DNA-binding activity of the HTH domain, depending on the nature of the bound effector. It has been suggested that NAD acts as the co-repressor of NadR: as shown in Figure 3, when NAD intracellular level increases, NAD binds to NadR promoting its binding to DNA, and so the transcription of the biosynthetic genes is repressed. On the other hand, when NAD level decrease and ATP is available, the NAD binding site in the NadR protein is occupied by ATP that operates as an anti-repressor, promoting dissociation of NadR from DNA and so promoting transcription.

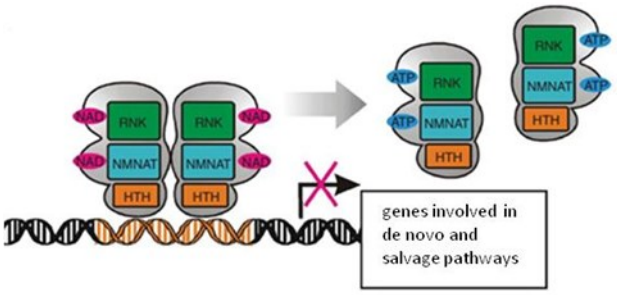

Figure 3: Regulation mechanism of NadR transcription factor. Adapted from: Sorci, L., Kurnasov, O., Rodionov, D. A., & Osterman, A. L. (2010). Genomics and enzymology of NAD biosynthesis.

1.5.2 NiaR

NiaR or niacin repressor operates as a Na-responsive transcriptional repressor of the *de novo* synthesis and salvage pathways in the Bacillales order (Rossolillo *et al.,* 2005). In *Streptococcus* and *Thermotoga* species, NiaR modulates the vitamin B3 uptake, acting as a repressor of a niacin transporter gene. This TF is present in bacteria from the *Bacillus* and *Clostridium* group and it is also present in the Thermotogales lineage and in *Fusobacterium nucleatum*. NiaR binds to a 22-bp palindromic DNA-binding motif conserved upstream of the NAD biosynthetic genes in all representatives of the *Firmicutes* group, whereas in the Thermotogales lineage, a distinct 17-bp palindromic DNA binding motif was identified (Rodionov *et al.,* 2008a).

The 3D structure of *T. maritima* NiaR showed a domain organization comprising a N-terminal HTH domain and a C-terminal domain that contains three conserved His residues involved in the binding of the Na effector (Weekes *et al.,* 2007). Na acts as the co-repressor: as shown in Figure 4, Na binds NiaR when its concentration increases, allowing the TF to block gene transcription; when the concentration of Na decreases, NiaR dissociates from DNA and transcription is promoted.

Figure 4: Regulation mechanism of NiaR transcription factor. Adapted from: Sorci, L., Kurnasov, O., Rodionov, D. A., & Osterman, A. L. (2010). Genomics and enzymology of NAD biosynthesis.

1.5.3 NrtR

NrtR (Nudix-related transcriptional Regulator) is a repressor controlling the transcription of genes involved in the *de novo* NAD biosynthesis, salvage pathways, and niacin uptake (Rodionov *et al.,* 2008b). This TF is responsible of the regulation of NAD biosynthesis in the majority of bacteria (Rodionov *et al.,* 2008b). Members of the NrtR family possess an N-terminal Nudix-like domain and a C-terminal DNA-binding domain with the characteristic winged HTH-fold (Haung *et al.,* 2009). NrtR binds to substantially variable DNA sequences. Most of them share a 21-bp palindrome symmetry and a conserved core with consensus GT-N7-AC. ADP-ribose, a NAD catabolite that signals the presence in the cell of a high NAD turnover, was found to suppress the *in vitro* binding of NrtR to DNA. It can be hypothesized that when intracellular ADP-ribose increases, it binds to NrtR and promotes the dissociation of the TF from DNA, allowing transcription of NAD biosynthetic genes (Figure 5).

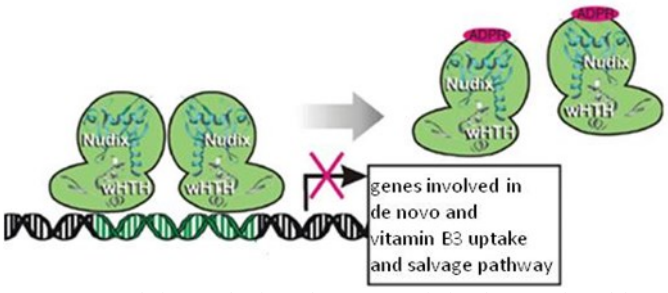

Figure 5: Regulation mechanism of NrtR transcription factor. Adapted from: Sorci, L., Kurnasov, O., Rodionov, D. A., & Osterman, A. L. (2010). Genomics and enzymology of NAD biosynthesis.

1.5.4 NadQ

NadQ regulator (COG4111) is the least characterized among the TFs of NAD biosynthesis. *In silico* studies have shown that NadQ protein possesses a domain architecture similar to that of members of the NrtR family, with a N-terminal Nudix-like domain and a C-terminal HTH domain (Brickman *et al.,* 2016; Leyn *et al.,* 2016). However, the NadQ and NrtR Nudix-like domains share little sequence similarity. NadQ was identified in most α-proteobacteria (*Rhizobiales*, *Rhodobacterales*, *Rhodospirillales*, *Caulobacterales*), some β-proteobacteria (*Burkholderiales*, *Neisseriales* including pathogenic species like *Bordetella* and *Neisseria*) and γ-proteobacteria (*Moraxellaceae*) (Rodionov *et al.,* 2008b).

In these bacteria, the reconstructed NadQ regulon includes the genes *nadA, nadB* and *nadC* that control the first three steps of *de novo* NAD biosynthesis. Moreover, in the *Rhodobacterales* and *Caulobacterales*, the NadQ regulon also comprises genes common to both the *de novo* and salvage pathway (*nadE* and *nadD*) (Leyn *et al.,* 2016).

By using comparative genomic techniques, a conserved 21-bp palindromic DNA motif (Figure 6) has been predicted as the NadQ binding site (Leyn *et al.,* 2016; Rodionov, 2007).

Figure 6: Representation of the NadQ binding site consensus sequence.

In 2016, Brickman *et al.,* demonstrated that in *Bordetella* species NadQ acts as a transcriptional repressor of the *nadC* gene, that codes for the enzyme QAPRT, the rate limiting enzyme in the conversion of QA to NAD and hypothesized that Na might be the effector molecule. In the same work, the authors reported that in most *Bordetella* genomes the *nadC* gene is likely co-transcribed with the *bug69* gene that encodes a small protein of the periplasmic binding protein family, predicted to be a transporter of QA. In this view, NadQ would be able to control simultaneously QA uptake and its conversion to NAD.

2. AIM OF THE RESEARCH

Reported evidence indicates that in PGPRs the synthesis of the biologically active form of vitamin B3, *i.e.* the coenzyme NAD, is directly involved in the ability of bacteria to promote plant growth. Therefore, the study of the regulation of the NAD biosynthetic pathway in these bacteria might improve our knowledge on PGPR-plant interactions, thus providing important information that might be instrumental to improve plant growth and health. In this work, we focused on the characterization of the transcriptional regulator that controls NAD biosynthesis in the majority of PGPR species, with the aim to shed light on its mechanism of action. To this end, the research activity included i) bioinformatic analyses, comprising *in silico* metabolic reconstruction and genomic context analysis, to identify the regulator; ii) the biochemical characterization of the regulator and the identification of the ligand which acts as the effector molecule; iii) the determination of the three-dimensional structure of the regulator.

3. MATERIALS AND METHODS

3.1 Bioinformatic analysis

Vitamin B3 metabolic pathways were analyzed by using the "NAD and NADP cofactor biosynthesis global" and "NAD regulation" subsystems at the SEED Viewer database (Overbeek *et al.,* 2005). In alternative, MicrobesOnline (Dehal *et al.,* 2009) was used as resource for comparative and functional genome analysis; the portal includes most complete genomes of bacteria. BLASTp servers provided by the National Center for Biotechnology Information at the National Library of Medicine were used for the analysis of sequenced genomes. 3D-BLAST servers were used for investigating the structural homology between NadQ and the whole protein structure database.

3.2 Cloning, expression and purification of NadQ

In order to produce NadQ recombinant protein, the encoding gene was amplified from *Agrobacterium thumefaciens* C58 (NC_003062) genomic DNA through PCR by using the primers reported in Table 2(A). The amplified sequence was cloned into pET100-TOPO vector (Invitrogen), in accordance with the manufacturer's instruction, to produce a fusion protein with six N-terminal histidine residues and an enterokinase protease cleavage site between the His-Tag and the first amino acid of native NadQ protein. The recombinant plasmid was sequenced at BMR Genomics (DNA Sequencing Service of Padova University, Italy, http://www.bmr-genomics.it/) before being transformed into *E. coli* BL21 (DE3) strain (Invitrogen), which carries an IPTG-inducible promoter for T7 polymerase in its chromosome.

Recombinant NadQ was produced by inoculating an overnight culture of freshly transformed cells in Luria Bertani (LB) medium supplemented with 100 μg/ml ampicillin. The culture was incubated at 37 °C with rotatory shaking (150 rpm). After reaching an OD_{600} of 0.6, the culture was placed at 23°C and after 20 min, protein expression was induced by adding 1mM IPTG. After overnight incubation (15h), induced cells were harvested by centrifugation (5,000g for 8min at 4°C) and resuspended in one-twentieth of the original culture volume of lysis buffer (50 mM Hepes/NaOH pH 7.5, 300 mM NaCl, 1 mM PSMF, protease inhibitor cocktail (Sigma)). Cells were disrupted by two

passages in a French pressure cell (18000psi), and the cell debris was removed by centrifugation (20 min at 20,000g at 4°C). The supernatant represents the crude extract. The recombinant protein was purified to homogeneity from the crude extract using an Äkta FPLC system equipped with a HisTrap FF IMAC (GE Healthcare) column (1ml) equilibrated with the equilibration buffer (50mM Hepes/NaOH pH 7.5, 300 mM NaCl) before loading the clarified cell lysate. Unbound proteins were removed by washing with 10 column volumes of equilibration buffer, followed by 15 column volumes of equilibration buffer containing 40mM imidazole. The elution of bound protein was carried out with 15 column volumes of a linear imidazole gradient from 40mM to 300mM, in equilibration buffer. All chromatographic steps were performed at room temperature. The NadQ protein eluted at ~250 mM imidazole and the purity were estimated to be higher than 95% through overloaded SDS-PAGE (Laemmli, 1970) and staining with Coomassie brilliant blue. The final protein concentration was determined with the Bradford method (Bradford, 1976) referring to a protein standard curve prepared with BSA. About 40 mg of pure protein was obtained starting from 1 liter of culture. The protein sample eluted from the IMAC column was subjected to gel filtration chromatography on Sephadex G-25 resin (GE Healthcare) in the equilibration buffer to remove imidazole. The final sample was aliquoted and stored at -20°C until use.

3.3 Gel filtration of NadQ

The native molecular weight of recombinant-NadQ was estimated by gel filtration chromatography through FPLC on a Superose 12 HR 10/30 column (GE Healthcare) equilibrated with 50mM Hepes/NaOH, pH 7.5, 300 mM NaCl. A calibration curve was generated using the following gel filtration standards: Carbonic Anhydrase (29 kDa), Ovalbumin (44 kDa), BSA (66 kDa) (Sigma).

3.4 DNA binding activity of NadQ

We first generated the DNA fragment containing the two DNA sequences in the upstream region of the *nadABC* operon that are predicted to be bound by NadQ. To this end, we amplified the region of interest via PCR, using the primers listed in Table 2(B) and the genomic DNA of *A. tumefaciens* as the template. The DNA fragment was then purified

using the High Pure PCR Product Purification kit (Roche, Basel, Switzerland), spectrophotometrically quantified and used in gel mobility shift assays.

For the electrophoretic mobility shift assay, 76 ng (800 pmol) of the DNA fragment were incubated with different amounts of NadQ in binding buffer consisting of 10mM Tris, pH 7.5, 50mM KCl, 2.5% glycerol, 5mM $MgCl_2$, 0.05% NP-40 and 0.5 mg/ml BSA, in a final volume of 20 µl. After 20 min at 25°C, samples were loaded on a 6% native polyacrylamide gel (30:0.8 acrylamide:N,N9-methylenebisacrylamide [w/w]). Electrophoresis was carried out in 0.5X TBE (Tris–Borate–EDTA) buffer for 60 min at 120 V, at 4°C. The gels were stained for 40 min in 1X TBE buffer, containing 2ul Sybr Green I diluted 1:10,000.

The electrophoretic mobility shift assay was performed with the His-tagged NadQ and the protein without its N-terminal tag. To remove the tag, the NadQ protein was desalted with G25 in 20mM Tris/HCl, pH 7.4, 1mM TCEP and incubated with enterokinase (Novagen), to a ratio of 1U of enzyme to 25 ug of protein, for 19 hours at 23°C. In order to purify the protein from the His-tag a gel filtration chromatography on Superose 12 was performed as described above, including 1mM TCEP in the elution buffer. The protein was aliquoted and stored at -20°C until use.

3.5 Crystallization of NadQ, Data Collection and Structure Determination

The purified protein was diluted five times with 50mM HEPES, pH 7.5 (at room temperature), in order to reduce the concentration of salts in solution. The sample was then concentrated using an Amicon Ultra Centrifugal Filter (cutoff 10 kDa, Merck, Millipore), at 18°C. The final protein concentration was 7 mg/ml. All crystallization attempts were carried out using the sitting drop vapor diffusion method. One microliter of NadQ solution was mixed with equal volume of reservoir solution and equilibrated against 100 µl of the reservoir solution. Different commercially available kits were used from JENA Bioscience. For the apo-NadQ, the best crystals were obtained in reservoir solution containing 150 mM di-Sodium DL-malate, pH 7.0, 20% (w/v) PEG 3350 (JCSG kit). Crystals grew to their final size in four-five months at 18°C.

For the NadQ-DNA co-crystallization trials, a 32 bp oligodeoxynucleotide duplex with sticky ends (Table 2C) was custom synthetized. The protein-dsDNA complex was formed by mixing NadQ and dsDNA at a 1:1.2 molar ratio. Crystals were grown after mixing equal volume of complex with reservoir solutions containing 100 mM HEPES, pH 7.5, 100 mM Lithium chloride, 5% (w/v) PEG 6000 (Classic-I kit). Crystals appeared after 7 days at 18°C.

.

For co-crystallization with NAD, NadQ was mixed with NAD at a 1:10 molar ratio. Putative NadQ-NAD crystals appeared in reservoir solution containing 150mM potassium sodium tartrate, 26% (w/v) PEG 3400. Crystals appeared after 35 days at 18°C with NAD, respectively.

The selenomethionine-substituted (SeMet) protein was produced as described (Ramakrishnan *et al.,* 1993). The same plasmid used to express the protein was transformed into *E coli* B834 (DE3), a methionine auxotrophic strain. The transformed cells were grown at 37°C in minimal medium M9 supplemented with ampicillin (100 ug/ml) and selenomethionine (40 ug/ml). After 12 hours at 37°C, *E. coli* cells reached an OD_{600} of 0.55. Protein expression was induced with 1mM IPTG and after 15 hours at 23°C, cells were collected. The purification was performed as previously described, with the exception of the presence of 1mM DTT in all buffers. About 13 mg of protein were obtained starting from 1 liter of culture. The concentrate SeMet-NadQ was co-crystallized with ATP at a 1:10 molar ratio. Crystals grew under conditions different from those used to produce native crystals: 100 mM Bis-Tris-Propane, pH 7.0, 250 mM sodium potassium tartrate, 24 % (w/v) PEG 3400. Crystals appeared after 2-3 months at 18°C to a size of 50 x 50 x 100 um^3.

Crystals were transported in plates at the various beamlines, mounted in nylon loops and flash-frozen directly at 100 ° K in a nitrogen gas stream. For NadQ-dsDNA the diffraction data were collected at the European Molecular Biology Laboratory (EMBL, Hamburg, Germany). For SeMet-NadQ-ATP crystals data were collected at Elettra Synchrotron (Trieste, Italy), and for the other crystals data were collected at the European Synchrotron Radiation Facility (ESRF, Grenoble, France).

The NadQ structures were solved by the SAD method using the selenium anomalous signal. Among the thirty SeMet crystals analyzed, only one was of sufficient quality to allow collection of a SAD dataset. The diffraction data were processed and scaled with the XDS/XSCALE program package. The crystals belong to space group P 2_1, with unit cell a=58.281 Å, b=134.346 Å, c=87.089 Å and α=90.00°, β=100.04°, γ=90.00°. The positions of 16 Se atoms (out of the 32 expected) were determined with SHELXD; the missing Se residues were located in the N-terminus of the recombinant protein comprising 36 residues that derive from the cloning procedure and were not defined in the electron density maps. SHELXE was used to refine the position of the Se sites and improve the electron density maps (Sheldrick, 2015). Automated model building was accomplished by CCP4 package (Collaborative, 1994), which allowed the partial building of the main chains of the four molecules (two dimers) of the symmetric unit. The manual fitting of the side chains and solvent molecules into electron density maps were performed using COOT (Emsley and Cowtan, 2004), PHENIX suite (Adams *et al.,* 2002) and Refmac5 (Murshudov *et al.,* 1997) of the CCP4 package, under the monitor of Rwork and Rfree, and of the Ramachandran plot (Laskowski *et al.,* 1993).

3.6 Cloning, expression and purification of Bug69 and Bug27

The genes encoding for Bug27 and Bug69 were amplified from genomic DNA of *Bordetella pertussis* Tohama I (NC_002929) with the primers reported in Table 2(A). Primers were designed to incorporate a *Nco*I restriction site at the 5' end of each gene, and a *Hind*III or *Xho*I restriction site at the 3' end of Bug27 or Bug69, respectively. The amplified sequences, encoding the mature part of the proteins without their signal peptides, were cloned into the pET28c vector. The constructs were used to transform *E. coli* BL21 (DE3) cells. The transformed cells were grown at 37°C in Luria Bertani medium supplemented with kanamycin (100 ug/ml). After reaching an OD_{600} of 0.7, cultures were shift at room temperature and after 20 min, proteins' expression was induced with 1mM IPTG and cells were grown at 23°C for 15 hours. All the following steps were performed at 4 °C. Cells were harvested by centrifugation (5,000g for 8 min), resuspended in 1/20 of the original culture volume in the lysis buffer (50 mM sodium phosphate, pH 8.0, 0.3 M NaCl, 5 mM imidazole) freshly supplemented with 1 mM PMSF and protease inhibitor cocktail. Cells were lysed by two passages through French Press (18,000 psi). The homogenates were clarified by centrifugation (20,000g for 25 min) for

subsequent purifications. Both His-tagged Bug-proteins were purified by NiNTA affinity chromatography. The clarified supernatants were loaded onto 1ml NiNTA columns (Qiagen) equilibrated with the lysis buffer. After washing with 20 mM imidazole in the same buffer, the elution of both recombinant proteins was obtained with imidazole concentration of 250 mM. Purification was monitored by SDS–PAGE according to Laemmli (Laemmli, 1970). Protein concentration was determined by the method of Bradford (Bradford, 1976), and about 9 mg of pure Bug27 and 5mg of pure Bug69 were obtained starting from 250 ml of cultures. Samples were stored at 4 °C.

3.7 Fluorescence-based thermal shift binding assay

The assay was adopted from a previously published method (Pantoliano *et al.,* 2001) and analyses were performed after denaturation and renaturation steps of proteins to remove endogenous ligands, as described for Bug27 (Herrou *et al.,* 2007). Briefly, the assay was carried out in a RotorGene 3000 real-time PCR, in a final assay volume of 25 µl. The assay mixture contained 1 µM of proteins, different concentrations of various compounds/substrates (dissolved in water) and 2.5X Sypro orange (Invitrogen) in 40 mM Tris/HCl, pH 8.0, 250 mM NaCl. The mixtures were pre-heated at 35°C for 5 min, then heated to 40°C in 15 sec, and finally heated from 40 to 99° C with a heating rate of 0.5°C every 5 sec. The fluorescence intensity was measured with Ex/Em: 470/585 nm. The melting temperature (Tm) was determined by taking the maximum point of the slope-derivative peak. Calculations were performed using GraphPad Prism version 7.00 for Windows, GraphPad Software (La Jolla California USA, www.graphpad.com).

	Primers name	Primers Sequence
(A)	*A. tumefaciens nadQ* fw	5′-CAACGTGACCATCGGGCTTGCCCAT-3′
	A. tumefaciens nadQ rev	5′-TCAATTGCGGGAGAGGGGCAGTTTCGT-3′
	B. pertussis Bug27 fw	5′-TAT**CCATGG**TTGCCACCGGCGACTTCCCG-3′
	B. pertussis Bug27 rev	5′-GCC**AAGCTT**GTCCACTTTCAGGCCGATCTGC-3′
	B. pertussis Bug69 fw	5′-TAT**CCATGG**TTGCGCCGGCCACCTATCCC-3′
	B. pertussis Bug69 rev	5′-AAA**CTCGAG**GTCGGCGCaGCCCCA-3′
(B)	*A. tumefaciens nadA* fw	5′-AGACCGTTCTTGATGAACG-3′
	A. tumefaciens nadA rev	5′-GCGGCTGAAATCTGCTC-3′
(C)	dsDNA for crystallization	5′- TTGAC*ATATGCTCACAATGAGAATAT*GTCTTC-3′ 3′-GAACTGTATACGAGTGTTACTCTTATACAGAA -5′

Table 2: Oligonucleotide primer sequences used for *genes* cloning (A), for gel mobility shift assays (B) and for crystallization of the NadQ-DNA complex (C). The added sequence for TOPO cloning is underlined. Restriction sites are in bold. The binding box of NadQ is in italic.

4. Results

4.1 *In silico* analysis of NAD biosynthesis and regulation in PGPRs

We focused on the reconstruction of the NAD biosynthetic machinery in the PGPRs described in Table 1 (Introduction section), which are most of the species whose genome has been fully sequenced and whose beneficial interaction with the host plant has been experimentally demonstrated. The results are shown Table 3.

Genera	Species	*de novo*	Na	Nam via Na	Nam via NMN	Nr
Acinetobacter	*baylyi*	+	+	+	+	
Agrobacterium	*tumefaciens*	+	+	+		
Arthrobacter	*chlorophenolicus*	+	+	+		+
Azotobacter	*vinelandii*	+	+	+		
Bacillus	*subtilis*	+	+	+		
Bradyrhizobium	*sp. BTAi1*	+	+	+		
Burkholderia	*phytofirmans strain PsJN*	+	+		+	
Enterobacter	*hormaechei ATCC 49162*	+	+	+		+
Klebsiella	*spp.*	+	+	+	+	+
Mesorhizobium	*spp.*	+	+	+		
Methylobacterium	*sp. PPFM-Ah*	+	+	+		
Nitrobacter	*spp.*	+	+			
Pseudomonas	*fluorescens Pf-5*	+	+	+		+
Rhizobium	*leguminosarum*	+	+	+		
Rhodopseudomonas	*palustris*	+	+	+		
Serratia	*marcescens*	+	+	+		+
Sinorhizobium	*meliloti*	+	+	+		

Table 3: NAD biosynthetic pathways in selected PGPRs.

All analyzed PGPRs can produce NAD both *de novo* and starting from Na. All of them, with the exception of *Nitrobacter sp.* can transform Nam to NAD, either via Na, and/or via NMN. Finally, half of these PGPRs can produce NAD starting from Nr.

The analysis showed that the *de novo* pathway is functional in all the selected PGPRs. This finding, together with the experimental evidence showing its involvement in the promotion of potato plant growth by *Burkolderia sp.* strain PsJN (Wang *et al.,* 2006), prompted us to focus our investigation on the regulation of this route. To this end, we have performed a bioinformatic analysis to search for the occurrence of known bacterial regulators of NAD biosynthesis in the selected PGPRs. We found that in all selected *Rhizobiales* NadQ was present (Table 4). Among these species, some are of particular

importance in agriculture, like *Sinorhizobium meliloti*, *Rhizobium leguminosarum* and *Mesorhizobium spp.*

Genera	Species	Regulator
Acinetobacter	*baylyi*	NrtR
Agrobacterium	*tumefaciens*	NadQ
Arthrobacter	*chlorophenolicus*	NrtR
Azotobacter	*vinelandii*	
Bacillus	*subtilis*	NiaR
Bradyrhizobium	*sp. BTAi1*	NadQ
Burkholderia	*phytofirmans strain PsJN*	
Enterobacter	*hormaechei ATCC 49162*	NadR
Klebsiella	*spp.*	NadR
Mesorhizobium	*spp.*	NadQ
Methylobacterium	*sp. PPFM-Ah*	NadQ
Nitrobacter	*spp.*	NadQ
Pseudomonas	*fluorescens Pf-5*	NrtR
Rhizobium	*leguminosarum*	NadQ
Rhodopseudomonas	*palustris*	NadQ
Serratia	*marcescens*	NadR
Sinorhizobium	*meliloti*	NadQ

Table 4: NAD biosynthesis transcription factors occurring in selected PGPRs.

It has been predicted that in *Rhizobiales*, NadQ controls the *de novo* NAD biosynthesis (Leyn *et al.,* 2016). Indeed, as shown in the genomic context analysis of *nadQ* gene in these species (Figure 7), the gene is mostly found close to the operon *nadABC,* supporting its involvement in the regulation of *de novo* NAD biosynthesis. Therefore we focused on the characterization of this regulator.

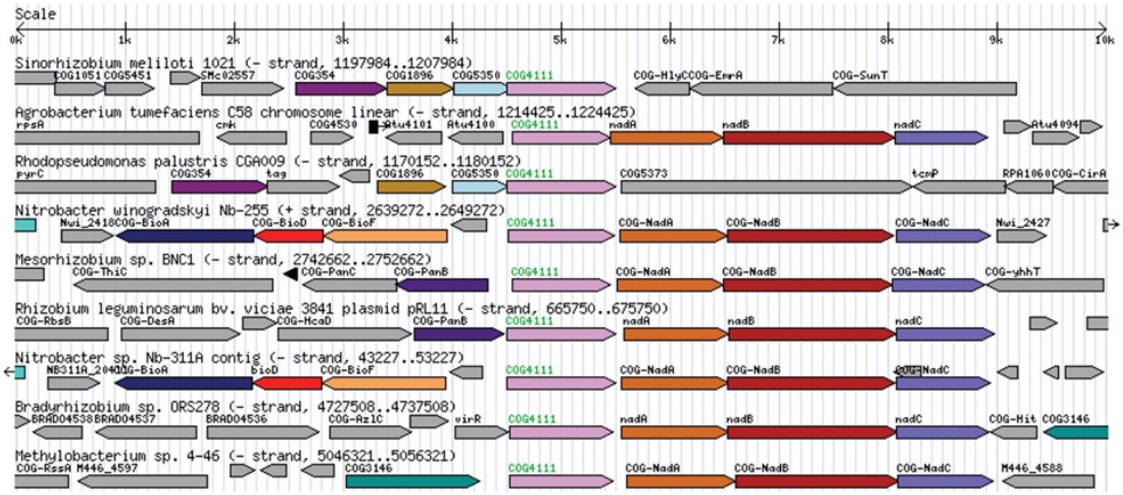

Figure 7: NadQ (COG4111) genomic context in PGPRs.

4.2 Expression, purification and molecular properties of *A. tumefaciens* NadQ

To give an insight into the regulatory function of NadQ, we produced the *Agrobacterium thumefaciens* C58 protein in recombinant form. The corresponding gene was cloned into a vector suitable for the overexpression in *E. coli* and the conditions for the expression of the recombinant protein were optimized. As shown in Figure 8A, the best expression of the protein was obtained after overnight induction of the culture at 23°C. The recombinant protein was purified to homogeneity by Ni^{2+}-chelating affinity chromatography, as described in Materials and Methods. Fractions from the different steps of the purification procedure were subjected to SDS-PAGE (Figure 8B). The pure protein showed a molecular mass of about 38.8 kDa, in agreement with the expected recombinant protein's size (Figure 8B). Gel filtration experiments showed a native molecular mass of about 58 kDa and the comparison of these results with those from the SDS-PAGE analysis suggests that in solution NadQ exists in equilibrium between a monomeric and a dimeric state (Figure 8C).

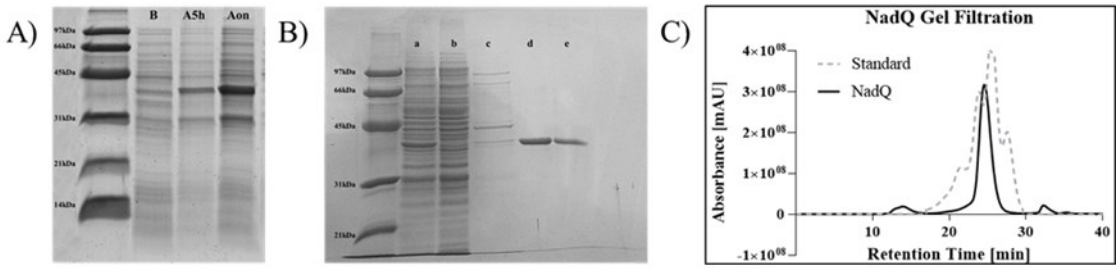

Figure 8: Expression and purification of NadQ protein. (A) SDS PAGE of extracts of *E. coli* cells transformed with the recombinant plasmid; B: Before induction; A5h: after 5 hour's induction; Aon: after overnight induction. (B) SDS PAGE of purification of recombinant NadQ protein. Fractions from the purification were : a) crude extract: b) flow through of the NiNTA column, c) column wash d) pool of eluted fractions e) final preparation. (C) Gel Filtration of pure NadQ protein. Used standards are: Carbonic Anhydrase (29 kDa), Ovalbumin (44kDa), BSA (66 kDa).

4.3 DNA binding properties of *A. tumefaciens* NadQ

An *in silico* analysis of the upstream region of the *nadABC* operon in *A. tumefaciens* allowed us to identify a possible NadQ binding site. We found that a region of 69 bp separated the *nadQ* coding sequence from that of *nadABC*. Here, based on the NadQ binding site consensus sequence (Rodionov, 2007) we predicted two binding sites (Figure 9). In order to experimentally validate the predicted DNA binding sites, we amplified a 151 bp fragment containing the two predicted motifs. This fragment comprises 128 bp of the upstream region of the operon sequence and the first 23 bp of the *nadA* sequence (Figure 9). Using electrophoretic mobility shift assay (EMSA), the purified NadQ protein was tested for its ability to bind this DNA fragment.

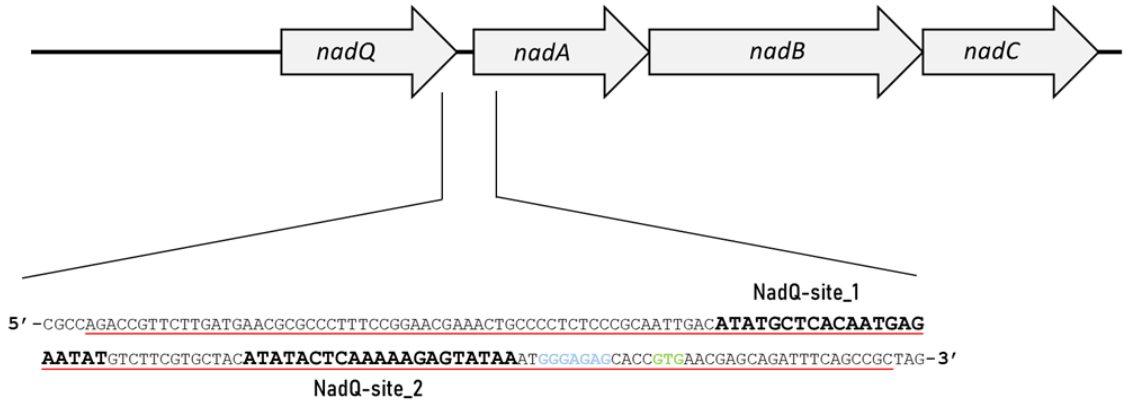

Figure 9: *Agrobacterium tumefaciens* NadQ regulon with the sequence of the region where two NadQ-binding sites (in bold) were predicted. The ribosome-binding site is in blue; the start codon of *nadA* gene is in green. The sequence of the 151 pb DNA fragment used for the EMSA is underlined in red.

As shown in Figure 10(A), a substantial shift of the specific DNA fragment of 151-bp was observed upon DNA incubation with the protein, which is indicative of the formation of the protein-DNA complex. Figure 10(A) shows that the intensity of the shifted DNA band increases in the presence of increasing amounts of NadQ. Notably, a DNA fragment

of 71-bp included in the incubation mixture as a negative control, was not affected by the presence of the protein, confirming the specificity of the NadQ–DNA interaction.

The effect of potential effectors of NadQ-DNA binding was tested by incubation of the protein with various intermediary metabolites associated with NAD biosynthetic pathways. The effect of ATP, NAD, NaAD, Na, NaMN, ADP and AMP, each one tested at 1mM concentrations, is shown in Figure 10(B). Among the tested metabolites, only ATP was able to prevent binding to DNA (Figure 10B). The effect was dose-dependent as shown in Figure 10(C). Subsequent investigations allowed us to discover that the effect of ATP was weakened by the presence of NAD (Figure 10D). These results were obtained both with the His-tagged NadQ and with the protein after removal of the tag with enterokinase. This implies that the tag of six histidine at the N-terminus of the protein does not interfere with the DNA binding ability.

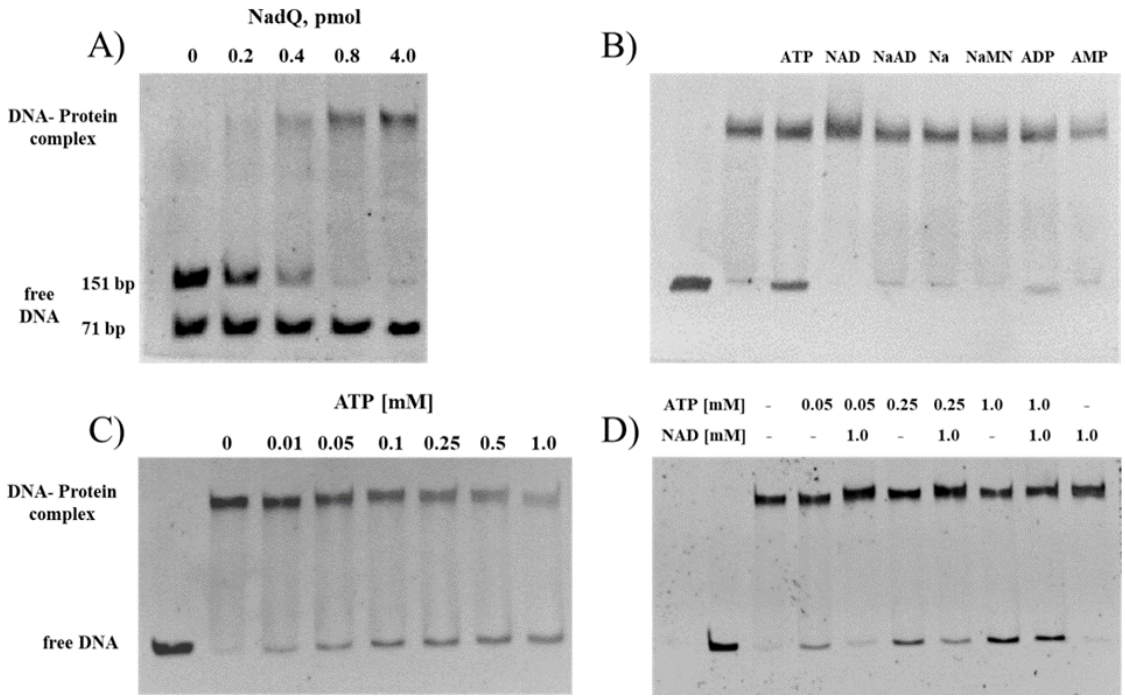

Figure 10: (A) Electrophoretic mobility of the 151 bp DNA fragment (0.8 pmol) incubated in the presence of the indicated amounts of NadQ. The specificity of interaction was confirmed by the lack of shift of the 71 bp fragment used as the control. (B) Mobility of the DNA fragment (lane 1) incubated with 4 pmol NadQ in the absence (lane 2) and in the presence of the indicated compounds at 1mM concentration (lanes 3-9). (C) Mobility of DNA incubated in the absence (lane 1) and in the presence of 4.0 pmol NadQ at the indicated concentrations of ATP (lanes 2-8). (D) Mobility of DNA incubated in the absence (lane 1) and in the presence of 4.0 pmol NadQ at the indicated ATP and NAD concentrations.

4.5 Resolution of *A. tumefaciens* NadQ structure

Based on the biochemical results, resolution of the 3D structure of NadQ in its apo-form and in complex with NAD or ATP or DNA might be helpful to clarify the mechanism of action of the regulator. To this end, we produced the selenomethionine-substituted (SeMet) NadQ, by expressing the protein in a methionine auxotrophic strain of *E. coli*, as reported in Material and Methods. The SeMet protein was purified as the native protein and the fractions from the different steps of the purification were analyzed through SDS-PAGE (Figure 11A). The purified protein possesses the same molecular weight of the native protein. We obtained crystals of SeMet-NadQ in complex with ATP and we acquired diffraction data at 2.05 Å resolution (Figure 11B).

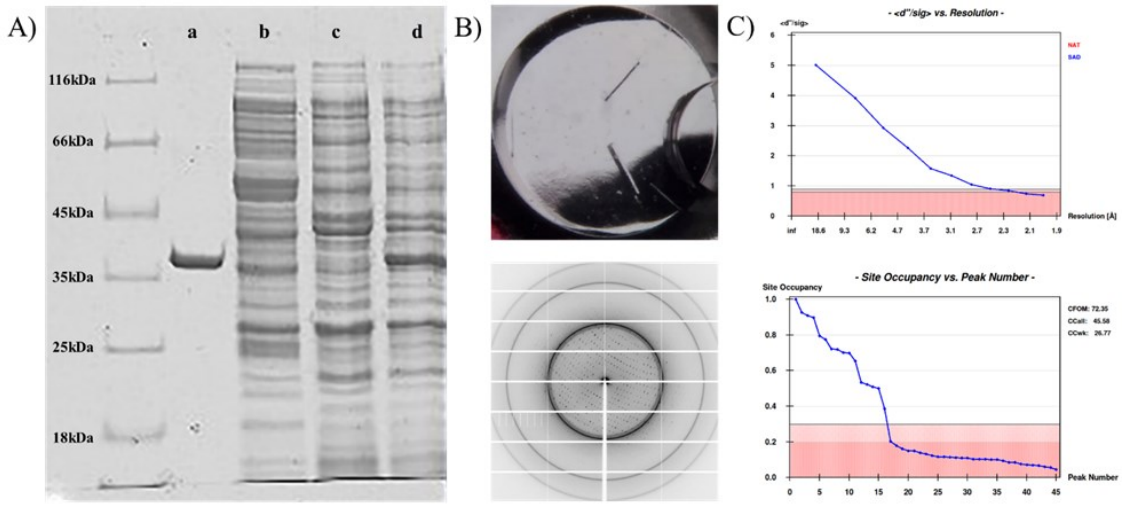

Figure 11: Purification and crystallization of the SeMet-NadQ protein. (A) SDS-PAGE of the purification: a) pool of fractions eluted from the NiNTA column, b) NiNTA column wash, c) flow-through of the NiNTA column, d) crude extract. (B) Crystals of the SeMet-NadQ-ATP complex (top) and the corresponding diffraction pattern (bottom). (C) SHELX statistic results for resolution and occupancy of Se atom sites.

We used the single-wavelength anomalous diffraction (SAD) technique to solve the structure of the complex. Since we were not able to obtain crystals of SeMet NadQ in its apo-form and in complex with NAD and DNA, crystallization trials were performed with the not-selenated protein. As shown in Figure 12, we acquired diffraction data from crystals of Apo-NadQ at 2.2 Å resolution, NadQ in complex with NAD at 2.1 Å resolution and the NadQ-DNA complex at 4.5 Å resolution.

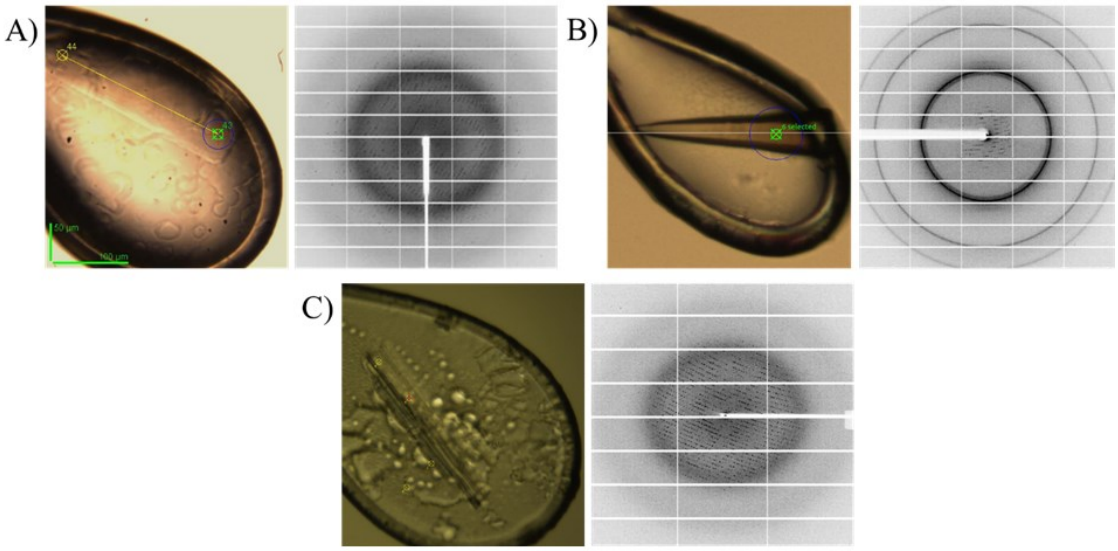

Figure 12: Crystals and their diffraction pattern: (A) Apo-NadQ; (B) NadQ-DNA complex; (C) NadQ- NAD complex.

4.5.1 Structure of apo-NadQ

The apo-NadQ structure was refined to R/R_{free} of 0.1943/0.2403 at 2.31 Å resolution; details of refinement statistics are reported in Table 5.

	apo-NadQ	SeMet-NadQ-ATP complex	NadQ-NAD complex	NadQ-DNA complex
Wavelength (Å)	0.97625	0.9797	0.87313	0.9763
Spacegroup	P 2_1	P 2_1	P 2_1	P 6_5
Cell parameters (Å, °)	a=58.3; b=133.3; c=86.8	a=58.28; b=134.35; c=87.09	a=57.89; b=131.99; c=86.23	a=103.4; b=103.4; c=152.34
Resolution range (Å)	48.51 – 2.31 (2.37-2.31)[a]	72.28 – 2.00 (2.071-2.00)[a]	43.99 – 2.11 (2.182-2.106)[a]	58.02 – 4.098 (4.224-4.098)[a]
Unique reflections	57061	84258	73368	7115
Multiplicity	3.8 (3.7)[a]	18.8 (12.8)[a]	6.7 (5.7)[a]	10.1 (7.2)[a]
Completeness (%)	99.7 (99.6)[a]	94.8 (66.87)[a]	99.66 (97.43)[a]	97.41 (73.98)[a]
Mean I/sigma(I)	9.3 (1.6)[a]	20.4 (1.5)[a]	5.0 (0.4)[a]	8.3 (0.8)[a]
R_{merge}	0.089 (0.728)[a]	0.122 (1.626)[a]	0.363 (5.493)[a]	0.182 (2.264)a
R_{pim}	0.08 (0.643)[a]	0.041 (0.674)[a]	0.23 (3.774)[a]	0.087 (1.249)a
CC1/2[a]	0.995 (0.520)[a]	0.999 (0.537)[a]	0.979 (0.098)[a]	0.998 (0.205)a
R-work	0.1943	0.2157	0.2373	0.279
R-free	0.2403	0.2501	0.2917	0.3969
Number of atoms	9774	10092	9608	
macromolecules	9368	9293	9342	
ligands	0	67	0	
water	406	732	276	
r.m.s.d.				
bond lenght	0.005	0.006	0.005	
angles	1.1	1.17	0.98	
Ramachandran				
favored (%)	94.89	94.42	93.99	
allowed (%)	4.76	4.77	5.74	
outliers (%)	0.35	0.8	0.27	
Molprobity clashcore	4.7	5.85	7.22	
Average B-factor	48.65	39.45	57.5	
macromolecules	48.75	39.21	57.52	
ligands	0	50.51	0	
solvent	46.24	41.52	50.75	

[a] Values in the highest resolution shell.

Table 5: Data collection and refinement statistics.

In the asymmetric unit of the apo-NadQ crystal, we found four molecules of NadQ corresponding to a dimer of dimers. The two dimers were almost identical, with an

r.m.s.d. of 0.570 Å. This is in agreement with the results from the gel filtration analysis showing that in solution NadQ was in equilibrium between monomeric and dimeric forms. Figure 13A shows the structure of NadQ dimer. Each monomer is composed of three domains (Figure 13B). The N-terminal domain (residues 1-148,) shows a Nudix hydrolase-like fold containing two α-helixes and a six β-stranded sheet (β1-β3, α1, β4-β6 and α2). It is very similar to the N-terminal domain of NrtR regulator from *Shewanella oneidensis* (Huang *et al.,* 2009) and AraR regulator from *Bacteroides thetaiotaomicron*, an L-arabinose-dependent TF which belongs to the NrtR family (Chang *et al.,* 2015) (Figure 14).

The central domain (residues 149-230) is composed by a four α-helical bundle (α3-α7), and is unique to NadQ. In the dimer, this domain of one monomer is stretched out to the adjacent monomer. The C-terminal domain (residues 231-328) is a winged helix-turn-helix (wHTH) DNA-binding domain, which is distantly related to several large families of bacterial TFs (Aravind 2005). It consists of a three α-helical bundle (α8-α10) followed by a long β-hairpin "wing" (β7- β8) and ending with an α-helix (α11) (Figure 13B), and superposes very well with the C-terminal domains of NrtR and AraR (Figure 14). As demonstrated for these regulators, the C-terminal domain of NadQ is predicted to bind the major groove surface of the DNA using the HTH motif, and the minor groove surface using the wing.

The first 34 residues at the N-terminus, deriving from the cloning procedure, as well as a loop region in the N-terminal domain (residue 77–80), were disordered.

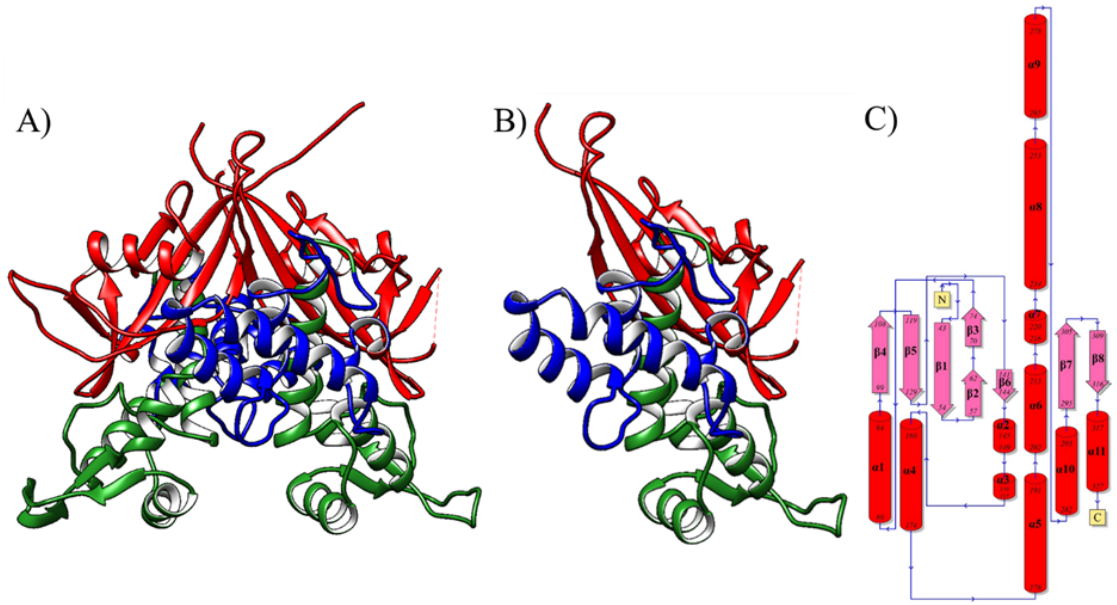

Figure 13: (A) Ribbon diagram of NadQ dimeric structure: the N-terminal domain is colored in red, the central domain is colored in blue and the C-terminal domain is colored in green; (B) Ribbon diagram of NadQ monomeric structure; (C) Topology diagram of NadQ protein, the sheets and helices are represented in pink and red color respectively.

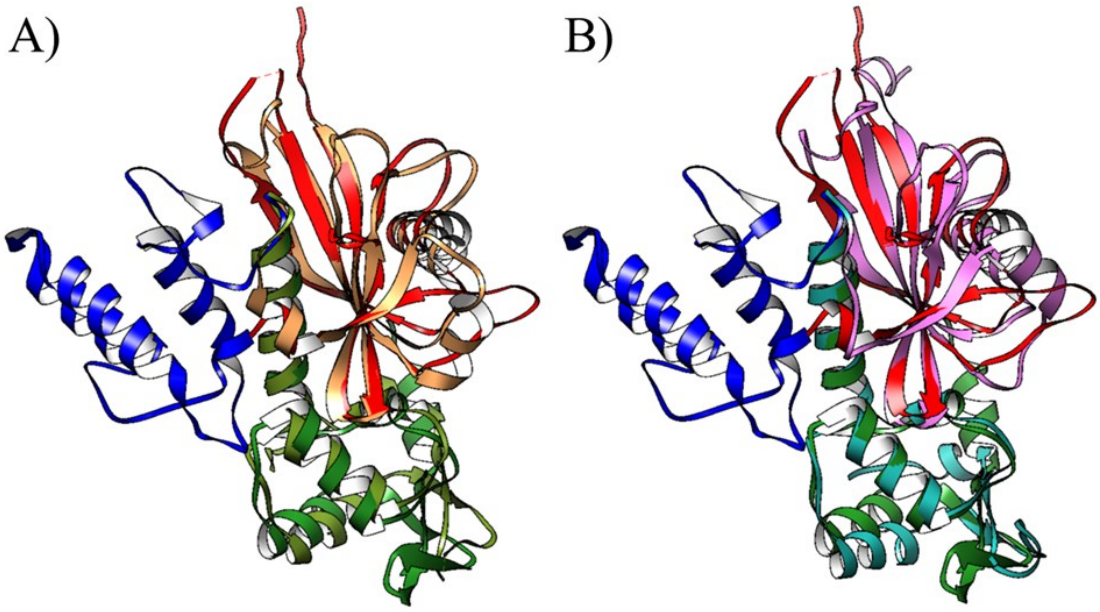

Figure 24: (A) Superposition of NadQ monomer with NrtR monomer structure (PDB entry 3GZ5); (B) Superposition of NadQ monomer with AraR monomer structure (PDB entry 5BS6).

4.5.2 Structure of NadQ-ATP complex

This structure was refined to R/R_{free} of 0.2157/0.2501 at 2.05 Å resolution (Table 5, Figure 15). As for the apo structure, we found two dimer molecules located in an asymmetric unit. The conformation of the two dimers in the ATP-bound NadQ were essentially identical (r.m.s.d. of 0.529 Å) and were also very similar to that of apo NadQ, with an r.m.s.d of 0.572 Å.

The ATP binding site is located at the interface between the two monomers in a region comprising the central domain of NadQ. It is formed by α-4, α-5, α-6 and β-6 of one monomer and α-1, β-6 and the C-terminal loop of the other monomer.

The adenine ring of ATP is sandwiched between the side chains of Arg237 and Tyr211 from the same subunit of the dimer (Figure 15). The two-hydroxyl groups of ribose are involved in an extensive hydrogen bond network with side chains of Arg186 and Glu212. The positively charged residue Arg109 forms salt bridges with the oxygen of the α-phosphate of ATP. The side chain of Thr80', Thr329', Tyr125'and Lys330', from the second subunit are hydrogen bonded to β- and γ-phosphate.

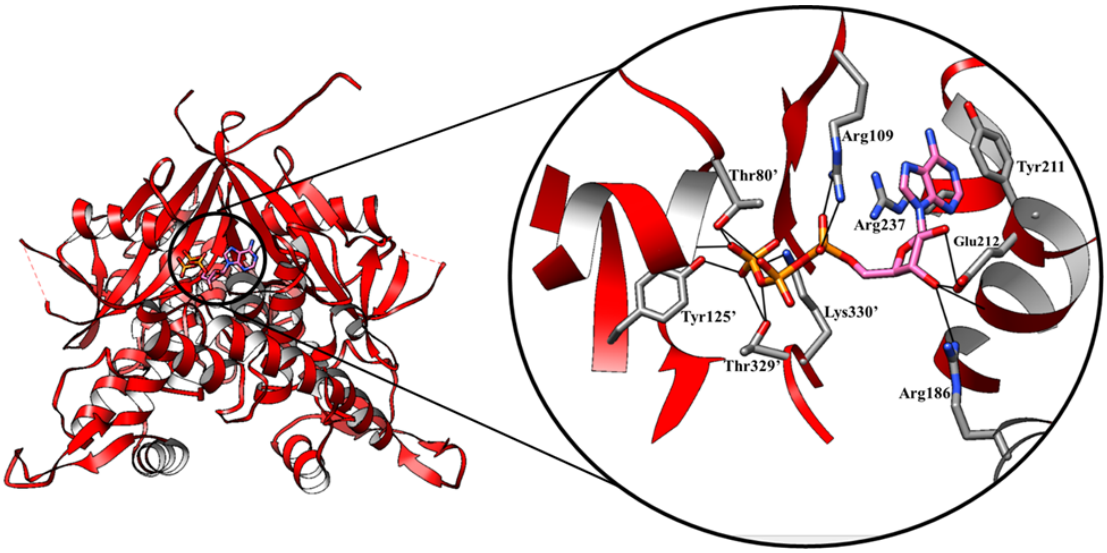

Figure 15: Ribbon diagram of NadQ dimeric structure with bound ATP. In the insert the ATP-binding pocket is shown, with the residues interacting with ATP represented as stick model and hydrogen bonds indicated as black lines.

4.5.3 Structure of NadQ-DNA complex

This structure was solved at 4.1 Å resolution (Table 5, Figure 16). The crystallographic asymmetric unit of this complex contained one NadQ dimer bound to a 32-bp DNA duplex. The HTH motif of the C-terminal domain of the protein interacts with the major groove surface of DNA, while the β-hairpin wing of the domain interacts with the minor groove. The 32-bp DNA duplex shows slight distortion from B-DNA conformation, causing both ends of the DNA to move toward the protein (Figure 16). The low resolution of the obtained data did not allow the identification of the amino-acids involved in DNA binding. Optimization of the crystallization conditions is required to solve the structure at higher resolution.

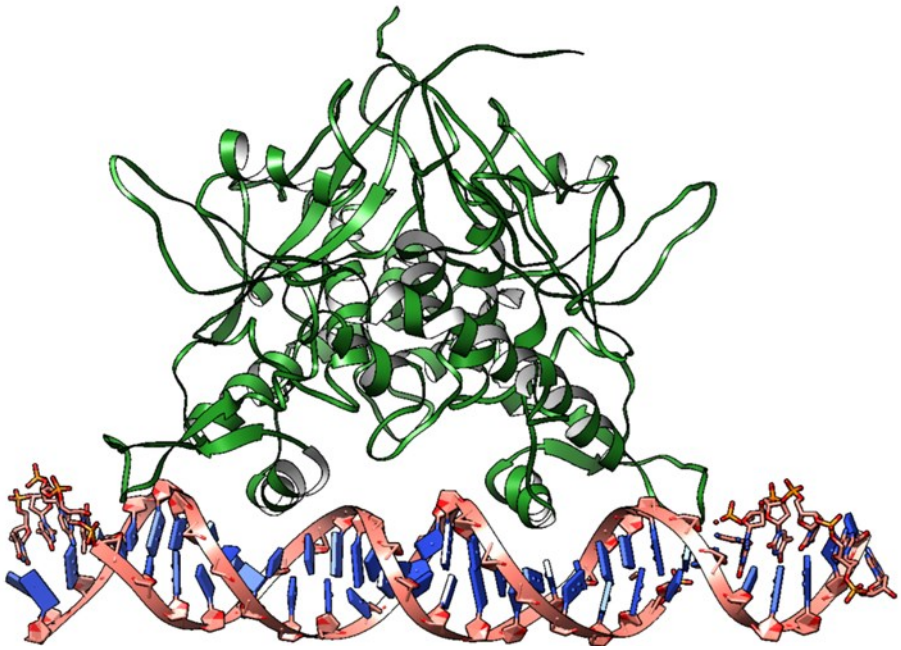

Figure 16: Overall structure of NadQ in complex with DNA double strands. NadQ is represented as ribbon diagram with dimer colored as green and specific double stranded DNA is represented as ribbon diagram with strands colored as pink.

The overall protein structure in the NadQ–DNA complex is quite distinct from the structures of apo-NadQ or NadQ bound to ATP (r.m.s.d. about 2.470 Å). Superposition of the ATP-bound and DNA-bound forms shows that ATP binding causes a conformational change in the entire C-terminal domain (Figure 17). The largest differences between the ATP-bound form and the NadQ–DNA complex are observed in the central domain, in the β-hairpin "wing" and the HTH motif of the C-terminal domain. Specifically, when ATP is bound it causes a movement in the region from α-4 to α-6 of the central domain that promotes rotation of the C-terminal domain, thus narrowing the distance between the two HTH motifs. Whereas such a distance in the NadQ-DNA complex allows a good fit into the major groove of the DNA duplex, this is no longer possible in the ATP-bound form.

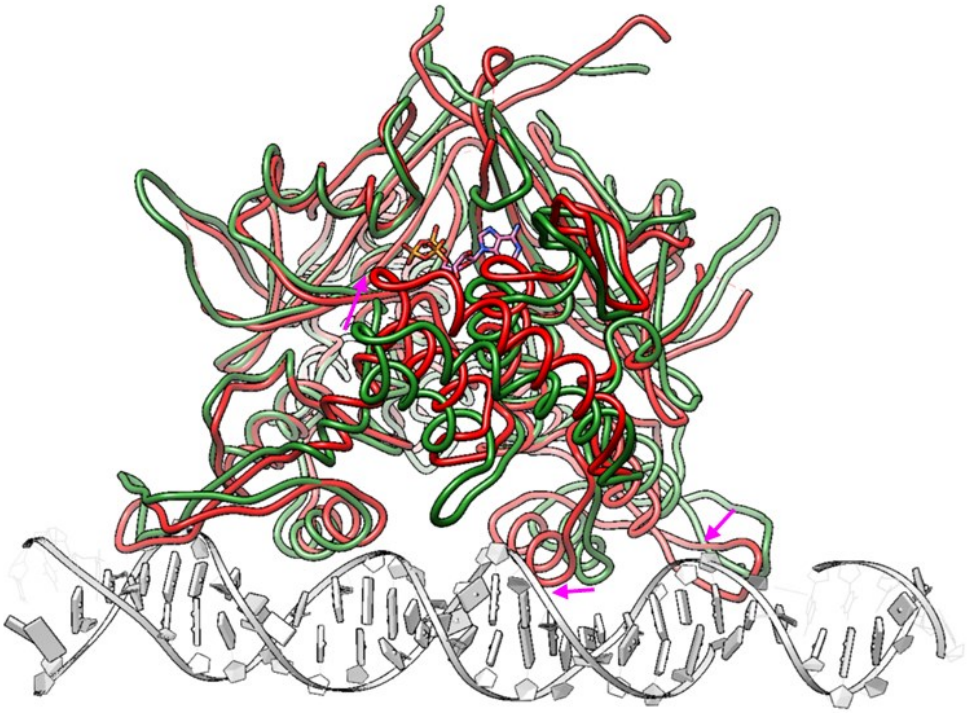

Figure 17: Structure comparison of NadQ-ATP and NadQ-DNA complexes. The ATP-bound structure is colored in red, the protein structure in the complex with DNA is colored in green.

4.5.4 Structure of NadQ-NAD complex

This structure was solved at 2.11 Å resolution (Table 5). As for the apo-NadQ and ATP-bound structures, we found two dimer molecules located in an asymmetric unit. The conformation of the two dimers in the "NAD-bound NadQ" were essentially identical (r.m.s.d. of 0.635 Å) and were also very similar to that of apo-NadQ, with an r.m.s.d of 0.578 Å.

Although the electron-map was refined to R/R_{free} of 0.2373/0.2917, we didn't observe any electron density corresponding to a NAD molecule. Different crystallization conditions should be tested in the presence of NAD to obtain the complex.

4.6 Characterization of *B. pertussis* Bug69

To shed more light on the biological function of NadQ, we focused on NadQ regulons in bacterial species other than PGPRs, like *Bordetella*. In fact, in some *Bordetella* species NadQ regulon comprises the gene *nadC* of the *de novo* NAD biosynthesis and the gene *bug69* coding for a protein of the periplasmic binding family (Figure18). This family comprises a broad range of proteins involved in the binding of different small molecules (like ions, vitamin, carbohydrates, amino acids) for their delivery to a protein membrane

transporter for import into the cytoplasm (Felder *et al.,* 1999). Since these *Bordetella* species do not have NadA and NadB, i.e. the first two enzymes of the *de novo* NAD biosynthesis, and NadC is the first enzyme involved in the conversion of QA to NAD (Figure 2A, Introduction section), the most plausible hypothesis is that Bug69 might be involved in QA uptake (Brickman *et al.,* 2016). However, it has been shown that inactivation of *bug69* in *Bordetella bronchiseptica* did not result in the expected phenotype, i.e. the inability to grow on QA, indicating that either Bug69 it is not involved in QA transport, or there are alternative QA transporters in this bacterium (Brickman *et al.,* 2016). A likely candidate for this role is Bug27, which shares 54.8% identity with Bug69 and is described to bind *in vitro* several compounds, including Na and Nam (Herrou *et al.,* 2007). No studies on the possible binding of Bug27 to QA have been reported. Therefore, the aim of this part of the thesis was to characterize the ability of Bug69 and Bug27 to bind QA.

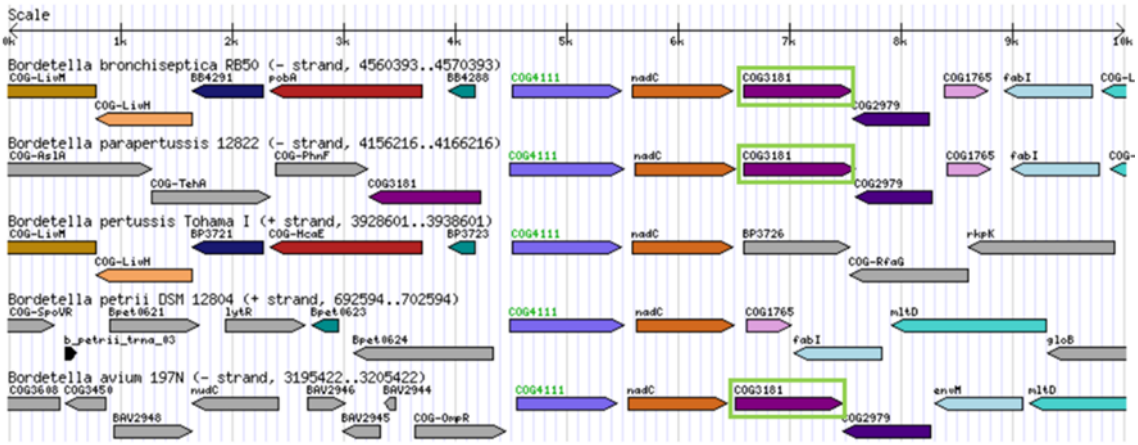

Figure 18: Genomic contest of nadQ (COG4111) gene in *Bordetella* species and location of *bug69* gene (COG3181, green boxes).

Due to the availability of *B. pertussis* genomic DNA we produced both proteins from *B. pertussis* in recombinant form, as described in Materials and Methods. The recombinant proteins resulting from our constructs carried a His-tag at the C-terminus for subsequent purification through affinity chromatography on a NiNTA resin. The purification was monitored by SDS-PAGE showing homogeneous final preparations, with expected molecular masses of 33.5 kDa for Bug69 and 32.9 kDa for Bug27, in agreement with the expected recombinant proteins' sizes (Figure 19).

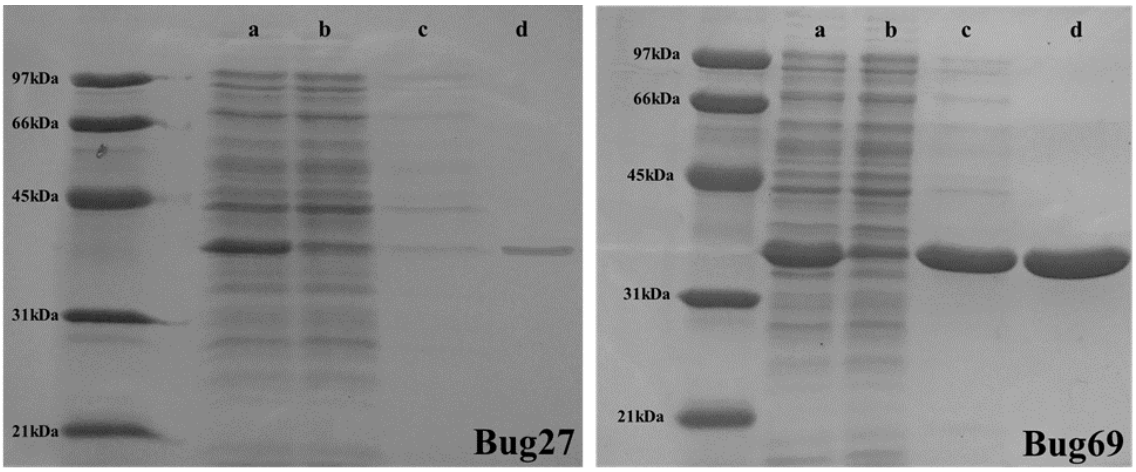

Figure 19: SDS PAGE of purification of recombinant Bug proteins. Fractions from the purification were: a) crude extract: b) fraction not bound to the NiNTA column, c) column wash d) eluted pool.

We then used a thermal shift assay to screen QA and similar compounds as potential ligands. Figure 20 shows the experimental thermal unfolding curves of the proteins in the presence of 1 mM Na, QA, Nam, Picolinic acid (PA), Citric acid (CA), Phthalic acid (FA). Among the tested metabolites, only FA and QA were found to affect the thermal denaturation of the proteins.

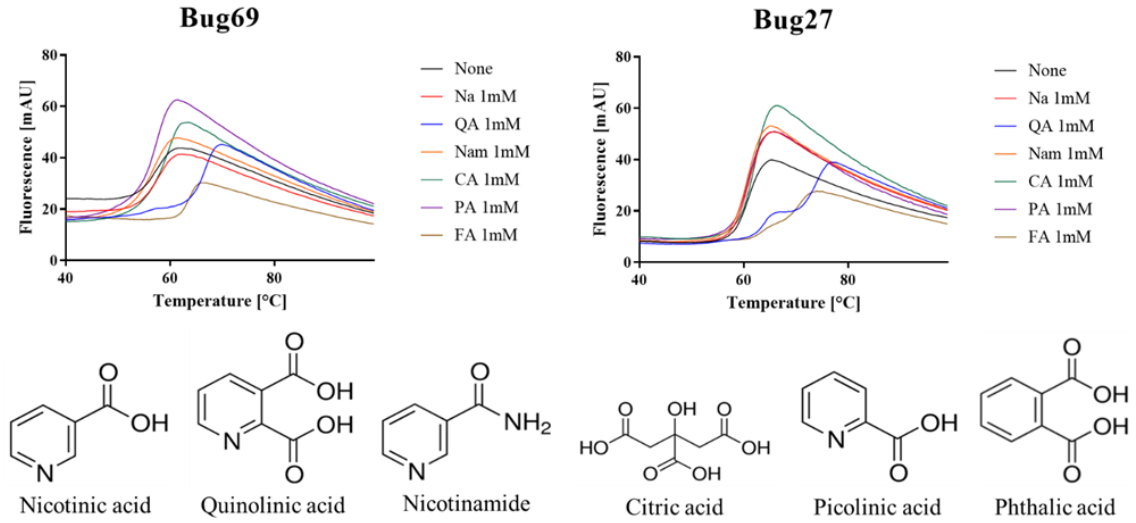

Figure 20: Thermal shift assay: denaturation curves obtained for Bug69 and Bug27 proteins in the presence of different compounds. The structures of the tested compounds is reported.

Their effect on the proteins' thermal stability (ΔTm) was analyzed at different concentrations of the compounds (Figure 21A). Binding affinity (Kd) values were calculated from the saturation kinetic profiles obtained by the thermal curves (Figure 21B). Both proteins exhibited Kd values for QA of about 5 µM. Kd values of 188 µM and 75 µM for FA were calculated for Bug69 and Bug27, respectively.

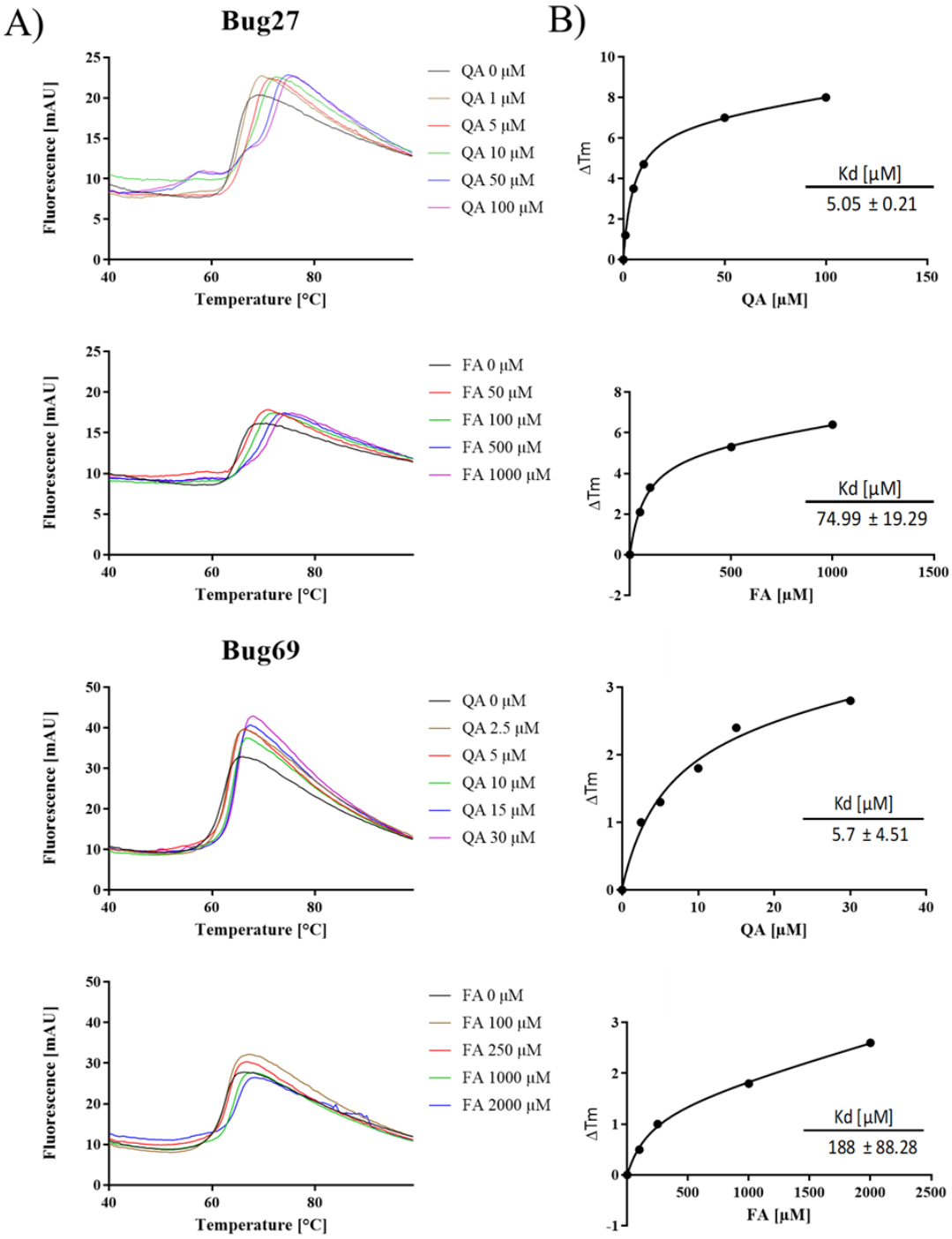

Figure 21: (A) Thermal Shift Assay denaturation curves obtained for Bug27 and Bug69 proteins in presence of different concentrations of quinolinic acid QA, or phathalic acid FA; (B) Saturation kinetic profiles for the calculation of the Kd values.

5. DISCUSSION

The *in silico* reconstruction of the NAD biosynthetic pathways in the bacterial species belonging to the PGPR group showed that the *de novo* synthesis pathway, starting from aspartate and dihydroxyacetone phosphate, is functioning in all selected PGPRs. In the majority of the analyzed PGPRs, such a pathway is controlled by the transcriptional regulator NadQ, which is the least characterized among the known regulators of bacterial NAD biosynthesis. *In silico* and *in vivo* studies have shown that NadQ acts as a repressor of genes coding for enzymes involved in the *de novo* NAD biosynthesis (Leyn *et al.,* 2016; Brickman *et al.,* 2016). Among them is the enzyme NadC that catalyzes the conversion of QA into NAMN, and has been shown to play an important role for the beneficial interaction between *Burkholderia phytofirmans* PsJN and potato (*Solanum tuberosum* L.) plants (Wang *et al.,* 2006; Sheibani-Tezerji *et al.,* 2015).

To shed light on the mechanism of action of the NadQ regulator, in this work we have produced the recombinant protein from *A. tumefaciens*, and we have experimentally validated its binding to a DNA region upstream of the operon involved in the first steps of the *de novo* NAD biosynthesis. Though mobility shift assays, we found that NadQ binds DNA in an ATP- and NAD-dependent manner. Specifically, ATP is able to prevent the formation of the NadQ-DNA complex, but its effect is abolished by the presence of NAD. These results support a working model for NadQ function which is shown in Figure 22.

In this model, when intracellular NAD levels increase, NAD binds NadQ, the regulator binds DNA and acts as repressor of the *de novo* synthesis. When NAD levels decrease and ATP is available, ATP displaces NAD and the complex dissociates from DNA, allowing biosynthetic genes transcription and thus NAD production. On the other hand, if NAD decreases but ATP levels are low, NadQ in its free form binds DNA and *de novo* NAD synthesis is stopped. We can assume that under physiological conditions, NAD regulates its own synthesis through the *de novo* route. If ATP is lowered, dihydroxyacetone phosphate is better used to fuel glycolysis rather than *de novo* synthesis. This route is therefore repressed and NAD can be formed starting from alternative sources, like vitamin B3, through the salvage pathways. This type of regulation closely resembles the mechanism of action of the transcription factor NadR

that also senses ATP and NAD to regulate NAD production in Enterobacteria (Grose *et al.,* 2005).

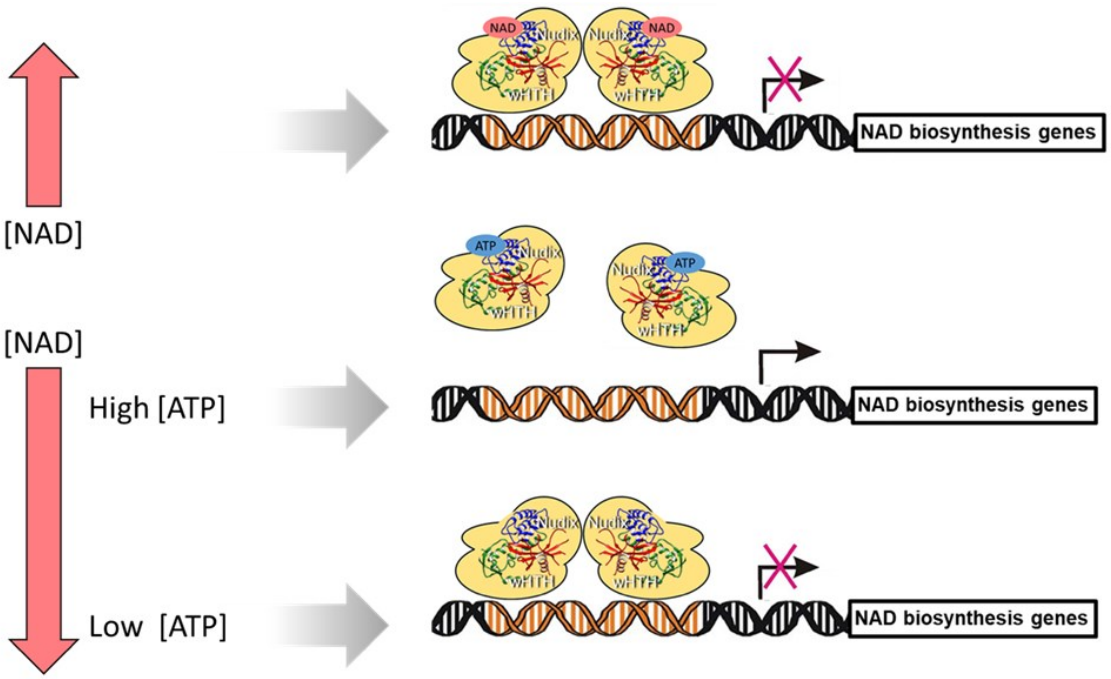

Figure 22: Possible mechanism of NadQ action.

To validate our model of NadQ mechanism, we have carried out crystallization trials to solve the 3D structure of NadQ through X-ray diffraction. We obtained diffraction data from crystals of the apo-protein, the protein in complex with DNA, ATP and NAD. We were able to solve and refine at high resolution the 3D structures of the apo-form, the NadQ-ATP and the NadQ-NAD complexes. The structural analysis revealed that NadQ consists of three domains: an N-terminal Nudix-like domain, a central domain which seems to be unique to NadQ, and a C-terminal wHTH DNA binding domain. Interestingly, the N-terminal domain is very similar to the N-terminal domain of regulators of the NrtR family. In these TFs the N-terminal domain binds the effector molecule, suggesting that it might have a similar function in NadQ. However, the 3D structure of the NadQ-ATP complex revealed that ATP binds in a cleft mostly formed by the central domain of the regulator. It is therefore tempting to speculate that the Nudix-like domain might bind the NAD molecule. Unfortunately, the structure of the NadQ-NAD complex did not show any NAD molecule bound to the protein. We also solved the structure of NadQ in complex with DNA, although at low resolution and therefore without the possibility to identify the amino-acids involved in the binding to DNA. Nevertheless,

superposition of the structures of NadQ-DNA and NadQ-ATP complexes provided a first view of the structural mechanism for the release of the protein from DNA: the movement of several secondary structure elements in the central domain of NadQ upon ATP binding results in the rotation of the C-terminal, leading to disruption of the protein–DNA interaction.

In this thesis, we have also shown that in *Bordetella* species, NadQ controls both the transport of QA across the cellular membrane and its conversion to NAD. In fact, we have found that in most species the NadQ regulon comprises *nadC* and *bug69*, the latter coding for a small protein, member of the periplasmic binding family. Characterization of Bug 69 from *B. pertussis* revealed that it is able to bind QA *in vitro* with an association constant in the low micromolar range.

6. CONCLUSIONS

It has been demonstrated that a properly regulated NAD biosynthetic pathway is indispensable for the metabolism, fitness and virulence of some bacteria, like *Pseudomonas aeruginosa* or *Bordetella pertussis*. Since, the *de novo* NAD biosynthetic route has been demonstrated to play an important role in the beneficial interaction between PGPRs and plants, we might assume that a properly regulation of the route is a key factor for the plant growth promotion by bacteria. Therefore, stimulation of NAD biosynthesis in these bacteria might improve plant colonization and growth.

In this work we have characterized the NadQ regulator which controls *de novo* NAD biosynthesis in most *Rhizobiales* of agricultural interest. We have demonstrated that it regulates NAD production by sensing the intracellular levels of both NAD and ATP. The structural characterization of the regulator bound to ATP and DNA has provided the first hint to the understanding of the mechanism of its regulation. Such a knowledge might be instrumental to the development of molecular tools targeting the NAD biosynthetic pathway in bacteria of agricultural interest in order to improve plant growth and health.

7. REFERENCES

Adams, P. D., Grosse-Kunstleve, R. W., Hung, L. W., Ioerger, T. R., McCoy, A. J., Moriarty, N. W., ... & Terwilliger, T. C. (2002). PHENIX: building new software for automated crystallographic structure determination. Acta Crystallographica Section D: Biological Crystallography, 58(11), 1948-1954.

Ahemad, M., & Kibret, M. (2014). Mechanisms and applications of plant growth promoting rhizobacteria: current perspective. Journal of King saud University-science, 26(1), 1-20.

Alferez, F. M., Gerberich, K. M., Li, J. L., Zhang, Y., Graham, J. H., & Mou, Z. (2018). Exogenous Nicotinamide Adenine Dinucleotide Induces Resistance to Citrus Canker in Citrus. Frontiers in plant science, 9, 1472.

Antoun, H., & Kloepper, J. W. (2001). Plant growth promoting rhizobacteria. Encyclopedia of genetics. Eds. S Brenner and J Miller. pp, 1477-1480.

Apel, K., & Hirt, H. (2004). Reactive oxygen species: metabolism, oxidative stress, and signal transduction. Annu. Rev. Plant Biol., 55, 373-399.

Aravind, L., Anantharaman, V., Balaji, S., Babu, M. M., & Iyer, L. M. (2005). The many faces of the helix-turn-helix domain: transcription regulation and beyond. FEMS microbiology reviews, 29(2), 231-262.

Arzanesh, M. H., Alikhani, H. A., Khavazi, K., Rahimian, H. A., & Miransari, M. (2011). Wheat (Triticum aestivum L.) growth enhancement by *Azospirillum sp.* under drought stress. World Journal of Microbiology and Biotechnology, 27(2), 197-205.

Asensi-Fabado, M. A., & Munné-Bosch, S. (2010). Vitamins in plants: occurrence, biosynthesis and antioxidant function. Trends in plant science, 15(10), 582-592.

Ashihara, H., Ludwig, I. A., Katahira, R., Yokota, T., Fujimura, T., & Crozier, A. (2015). Trigonelline and related nicotinic acid metabolites: occurrence, biosynthesis, taxonomic considerations, and their roles in planta and in human health. Phytochemistry reviews, 14(5), 765-798.

Azcón, R., & Barea, J. M. (1975). Synthesis of auxins, gibberellins and cytokinins by *Azotobacter vinelandii* and *Azotobacter beijerinckii* related to effects produced on tomato plants. Plant and Soil, 43(1-3), 609-619.

Barazani, O. Z., & Friedman, J. (1999). Is IAA the major root growth factor secreted from plant-growth-mediating bacteria?. Journal of Chemical Ecology, 25(10), 2397-2406.

Bhattacharyya, P. N., & Jha, D. K. (2012). Plant growth-promoting rhizobacteria (PGPR): emergence in agriculture. World Journal of Microbiology and Biotechnology, 28(4), 1327-1350.

Bradford, M. M. (1976). A rapid and sensitive method for the quantitation of microgram quantities of protein utilizing the principle of protein-dye binding. Analytical biochemistry, 72(1-2), 248-254.

Brenner, C. (2005). Evolution of NAD biosynthetic enzymes. Structure, 13(9), 1239-1240.

Brickman, T. J., Suhadolc, R. J., McKelvey, P. J., & Armstrong, S. K. (2017). Essential role of *Bordetella* NadC in a quinolinate salvage pathway for NAD biosynthesis. Molecular microbiology, 103(3), 423-438.

Burd, G. I., Dixon, D. G., & Glick, B. R. (2000). Plant growth-promoting bacteria that decrease heavy metal toxicity in plants. Canadian journal of microbiology, 46(3), 237-245.

Chaintreuil, C., Giraud, E., Prin, Y., Lorquin, J., Bâ, A., Gillis, M., ... & Dreyfus, B. (2000). Photosynthetic bradyrhizobia are natural endophytes of the African wild rice *Oryza breviligulata*. Appl. Environ. Microbiol., 66(12), 5437-5447.

Chang, C., Tesar, C., Li, X., Kim, Y., Rodionov, D. A., & Joachimiak, A. (2015). A novel transcriptional regulator of L-arabinose utilization in human gut bacteria. Nucleic acids research, 43(21), 10546-10559.

Cocking, E. C. (2003). Endophytic colonization of plant roots by nitrogen-fixing bacteria. Plant and soil, 252(1), 169-175.

Collaborative, C. P. (1994). The CCP4 suite: programs for protein crystallography. Acta crystallographica. Section D, Biological crystallography, 50(Pt 5), 760

Crawford, N. M., & Guo, F. Q. (2005). New insights into nitric oxide metabolism and regulatory functions. Trends in plant science, 10(4), 195-200.

Dardanelli, M. S., Carletti, S. M., Paulucci, N. S., Medeot, D. B., Caceres, E. R., Vita, F. A., ... & Garcia, M. B. (2010). Benefits of plant growth-promoting rhizobacteria and rhizobia in agriculture. In Plant growth and health promoting bacteria (pp. 1-20). Springer, Berlin, Heidelberg.

Dehal, P. S., Joachimiak, M. P., Price, M. N., Bates, J. T., Baumohl, J. K., Chivian, D., ... & Dubchak, I. L. (2009). MicrobesOnline: an integrated portal for comparative and functional genomics. Nucleic acids research, 38(suppl_1), D396-D400.

Dell'Amico, E., Cavalca, L., & Andreoni, V. (2008). Improvement of *Brassica napus* growth under cadmium stress by cadmium-resistant rhizobacteria. Soil Biology and Biochemistry, 40(1), 74-84.

Deryło, M., & Skorupska, A. (1993). Enhancement of symbiotic nitrogen fixation by vitamin-secreting fluorescent *Pseudomonas*. Plant and Soil, 154(2), 211-217.

El-Khawas, H., & Adachi, K. (1999). Identification and quantification of auxins in culture media of *Azospirillum* and *Klebsiella* and their effect on rice roots. Biology and Fertility of Soils, 28(4), 377-381.

Emsley, P., & Cowtan, K. (2004). Coot: model-building tools for molecular graphics. Acta Crystallographica Section D: Biological Crystallography, 60(12), 2126-2132.

Felder, C. B., Graul, R. C., Lee, A. Y., Merkle, H. P., & Sadee, W. (1999). The Venus flytrap of periplasmic binding proteins: an ancient protein module present in multiple drug receptors. AAps pharmsci, 1(2), 7-26.

Fleischmann, R. D., Adams, M. D., White, O., Clayton, R. A., Kirkness, E. F., Kerlavage, A. R., ... & Merrick, J. M. (1995). Whole-genome random sequencing and assembly of *Haemophilus influenzae* Rd. Science, 269(5223), 496-512.

Frost, G. M., Yang, K. S., & Waller, G. R. (1967). Nicotinamide adenine dinucleotide as a precursor of nicotine in *Nicotiana rustica* L. Journal of Biological Chemistry, 242(5), 887-888.

Galleguillos, C., Aguirre, C., Barea, J. M., & Azcón, R. (2000). Growth promoting effect of two *Sinorhizobium meliloti* strains (a wild type and its genetically modified derivative) on a non-legume plant species in specific interaction with two arbuscular mycorrhizal fungi. Plant Science, 159(1), 57-63.

Gazzaniga, F., Stebbins, R., Chang, S. Z., McPeek, M. A., & Brenner, C. (2009). Microbial NAD metabolism: lessons from comparative genomics. Microbiol. Mol. Biol. Rev., 73(3), 529-541.

Gerasimova, A. V., & Gelfand, M. S. (2005). Evolution of the NadR regulon in Enterobacteriaceae. Journal of bioinformatics and computational biology, 3(04), 1007-1019.

Goswami, D., Thakker, J. N., & Dhandhukia, P. C. (2016). Portraying mechanics of plant growth promoting rhizobacteria (PGPR): A review. Cogent Food & Agriculture, 2(1), 1127500.

Govindasamy, V., Senthilkumar, M., Magheshwaran, V., Kumar, U., Bose, P., Sharma, V., & Annapurna, K. (2010). *Bacillus* and *Paenibacillus* spp.: potential PGPR for sustainable agriculture. In Plant growth and health promoting bacteria (pp. 333-364). Springer, Berlin, Heidelberg.

Graham, J. H., & Leite Jr, R. P. (2004). Lack of control of citrus canker by induced systemic resistance compounds. Plant Disease, 88(7), 745-750.

Grose, J. H., Bergthorsson, U., & Roth, J. R. (2005). Regulation of NAD synthesis by the trifunctional NadR protein of *Salmonella enterica*. Journal of bacteriology, 187(8), 2774-2782.

Guilfoyle, T. J., & Hagen, G. (2007). Auxin response factors. Current opinion in plant biology, 10(5), 453-460.

Hashida, S. N., Takahashi, H., & Uchimiya, H. (2009). The role of NAD biosynthesis in plant development and stress responses. Annals of botany, 103(6), 819-824.

Herrou, J., Bompard, C., Antoine, R., Leroy, A., Rucktooa, P., Hot, D., ... & Jacob-Dubuisson, F. (2007). Structure–based Mechanism of Ligand Binding for Periplasmic Solute-binding Protein of the Bug Family. Journal of molecular biology, 373(4), 954-964.

Huang, N., De Ingeniis, J., Galeazzi, L., Mancini, C., Korostelev, Y. D., Rakhmaninova, A. B., ... & Zhang, H. (2009). Structure and function of an ADP-ribose-dependent transcriptional regulator of NAD metabolism. Structure, 17(7), 939-951.

Huddedar, S. B., Shete, A. M., Tilekar, J. N., Gore, S. D., Dhavale, D. D., & Chopade, B. A. (2002). Isolation, characterization, and plasmid pUPI126-mediated indole-3-acetic acid production in *Acinetobacter* strains from rhizosphere of wheat. Applied biochemistry and biotechnology, 102(1-6), 21-39.

Ibiene, A. A., Agogbua, J. U., Okonko, I. O., & Nwachi, G. N. (2012). Plant growth promoting rhizobacteria (PGPR) as biofertilizer: Effect on growth of *Lycopersicum esculentus*. Journal of American Science, 8(2), 318-324.

Kantha, T., Kantachote, D., & Klongdee, N. (2015). Potential of biofertilizers from selected *Rhodopseudomonas palustris* strains to assist rice (*Oryza sativa* L. subsp. indica) growth under salt stress and to reduce greenhouse gas emissions. Annals of microbiology, 65(4), 2109-2118.

Kennedy, A.C., (2005). The rhizosphere. In: Sylvia, D.M., Hartel, P.G., Fuhrmann, J.J., Zuberer, D.A. (Eds.), Principles and Applications of Soil Microbiology, 2nd ed. Pearson-Prentice Hall, Upper Saddle River, NJ, pp. 242–262.

Kloepper, J. W. (2003, October). A review of mechanisms for plant growth promotion by PGPR. In 6th international PGPR workshop (Vol. 10, pp. 5-10).

Kloepper, J. W., & Ryu, C. M. (2006). Bacterial endophytes as elicitors of induced systemic resistance. In Microbial root endophytes (pp. 33-52). Springer, Berlin, Heidelberg.

Kraus, J., & Loper, J. E. (1992). Lack of evidence for a role of antifungal metabolite production by *Pseudomonas fluorescens* Pf-5 in biological control of Pythium damping-off of cucumber. Phytopathology, 82(3), 264-271.

Kurnasov, O. V., Polanuyer, B. M., Ananta, S., Sloutsky, R., Tam, A., Gerdes, S. Y., & Osterman, A. L. (2002). Ribosylnicotinamide kinase domain of NadR protein: identification and implications in NAD biosynthesis. Journal of bacteriology, 184(24), 6906-6917.

Kurnasov, O., Goral, V., Colabroy, K., Gerdes, S., Anantha, S., Osterman, A., & Begley, T. P. (2003). NAD biosynthesis: identification of the tryptophan to quinolinate pathway in bacteria. Chemistry & biology, 10(12), 1195-1204.

Laemmli, U. K. (1970). SDS-page Laemmli method. Nature, 227, 680-5.

Laskowski, R. A., MacArthur, M. W., Moss, D. S., & Thornton, J. M. (1993). PROCHECK: a program to check the stereochemical quality of protein structures. Journal of applied crystallography, 26(2), 283-291.

Leyn, S. A., Suvorova, I. A., Kazakov, A. E., Ravcheev, D. A., Stepanova, V. V., Novichkov, P. S., & Rodionov, D. A. (2016). Comparative genomics and evolution of transcriptional regulons in Proteobacteria. Microbial genomics, 2(7).

Ma, W., Guinel, F. C., & Glick, B. R. (2003). *Rhizobium leguminosarum* biovar viciae 1-aminocyclopropane-1-carboxylate deaminase promotes nodulation of pea plants. Appl. Environ. Microbiol., 69(8), 4396-4402.

Madhaiyan, M., Reddy, B. S., Anandham, R., Senthilkumar, M., Poonguzhali, S., Sundaram, S. P., & Sa, T. (2006). Plant growth–promoting *Methylobacterium* induces defense responses in groundnut (*Arachis hypogaea* L.) compared with rot pathogens. Current microbiology, 53(4), 270-276.

Mahalingam, R., Jambunathan, N., & Penaganti, A. (2007). Pyridine nucleotide homeostasis in plant development and stress. International Journal of Plant Developmental Biology, 1(2), 194-201.

Mano, J. I., Belles-Boix, E., Babiychuk, E., Inzé, D., Torii, Y., Hiraoka, E., ... & Kushnir, S. (2005). Protection against photooxidative injury of tobacco leaves by 2-alkenal reductase. Detoxication of lipid peroxide-derived reactive carbonyls. Plant physiology, 139(4), 1773-1783.

Marek-Kozaczuk, M., & Skorupska, A. (2001). Production of B-group vitamins by plant growth-promoting *Pseudomonas fluorescens* strain 267 and the importance of vitamins in the colonization and nodulation of red clover. Biology and fertility of soils, 33(2), 146-151.

Marek-Kozaczuk, M., Rogalski, J., & Skorupska, A. (2005). The *nadA* gene of *Pseudomonas fluorescens* PGPR strain 267.1. Current microbiology, 51(2), 122-126.

Martínez-Viveros, O., Jorquera, M. A., Crowley, D. E., Gajardo, G. M. L. M., & Mora, M. L. (2010). Mechanisms and practical considerations involved in plant growth promotion by rhizobacteria. Journal of soil science and plant nutrition, 10(3), 293-319.

Mayak, S., Tirosh, T., & Glick, B. R. (2004). Plant growth-promoting bacteria that confer resistance to water stress in tomatoes and peppers. Plant Science, 166(2), 525-530.

Miwa, A., Sawada, Y., Tamaoki, D., Hirai, M. Y., Kimura, M., Sato, K., & Nishiuchi, T. (2017). Nicotinamide mononucleotide and related metabolites induce disease resistance against fungal phytopathogens in *Arabidopsis* and barley. Scientific reports, 7(1), 6389.

Miyamoto, E., Watanabe, F., Takenaka, H., & NAKANO, Y. (2002). Uptake and physiological function of vitamin B12 in a photosynthetic unicellular *coccolithophorid* alga, *Pleurochrysis carterae*. Bioscience, biotechnology, and biochemistry, 66(1), 195-198.

Møller, I. M. (2001). Plant mitochondria and oxidative stress: electron transport, NADPH turnover, and metabolism of reactive oxygen species. Annual review of plant biology, 52(1), 561-591.

Murshudov, G. N., Skubák, P., Lebedev, A. A., Pannu, N. S., Steiner, R. A., Nicholls, R. A., ... & Vagin, A. A. (2011). REFMAC5 for the refinement of macromolecular crystal structures. Acta Crystallographica Section D: Biological Crystallography, 67(4), 355-367.

Noctor, G., Queval, G., & Gakière, B. (2006). NAD (P) synthesis and pyridine nucleotide cycling in plants and their potential importance in stress conditions. Journal of Experimental Botany, 57(8), 1603-1620.

Ordentlich, A., Elad, Y., & Chet, I. (1987). Rhizosphere colonization by *Serratia marcescens* for the control of *Sclerotium rolfsii*. Soil Biology and Biochemistry, 19(6), 747-751.

Overbeek, R., Begley, T., Butler, R. M., Choudhuri, J. V., Chuang, H. Y., Cohoon, M., ... & Fonstein, M. (2005). The subsystems approach to genome annotation and its use in the project to annotate 1000 genomes. Nucleic acids research, 33(17), 5691-5702.

Palacios, O. A., Bashan, Y., & de-Bashan, L. E. (2014). Proven and potential involvement of vitamins in interactions of plants with plant growth-promoting bacteria—an overview. Biology and fertility of soils, 50(3), 415-432.

Pantoliano, M. W., Petrella, E. C., Kwasnoski, J. D., Lobanov, V. S., Myslik, J., Graf, E., ... & Salemme, F. R. (2001). High-density miniaturized thermal shift assays as a general strategy for drug discovery. Journal of biomolecular screening, 6(6), 429-440.

Paré, P. W., Farag, M. A., Krishnamachari, V., Zhang, H., Ryu, C. M., & Kloepper, J. W. (2005). Elicitors and priming agents initiate plant defense responses. Photosynthesis Research, 85(2), 149-159.

Penfound, T., & Foster, J. W. (1996). Biosynthesis and recycling of NAD. *Escherichia coli* and *Salmonella*: cellular and molecular biology. ASM Press, Washington, DC, 721-730.

Penfound, T., & Foster, J. W. (1999). NAD-dependent DNA-binding activity of the bifunctional NadR regulator of *Salmonella typhimurium*. Journal of bacteriology, 181(2), 648-655.

Pétriacq, P., Ton, J., Patrit, O., Tcherkez, G., & Gakière, B. (2016). NAD acts as an integral regulator of multiple defense layers. Plant physiology, 172(3), 1465-1479.

Raffaelli, N., Lorenzi, T., Mariani, P. L., Emanuelli, M., Amici, A., Ruggieri, S., & Magni, G. (1999). The *Escherichia coli* NadR regulator is endowed with nicotinamide mononucleotide adenylyltransferase activity. Journal of bacteriology, 181(17), 5509-5511.

Ramakrishnan, V., Finch, J. T., Graziano, V., Lee, P. L., & Sweet, R. M. (1993). Crystal structure of globular domain of histone H5 and its implications for nucleosome binding. Nature, 362(6417), 219.

Requena, N., Jimenez, I., Toro, M., & Barea, J. M. (1997). Interactions between plant-growth-promoting rhizobacteria (PGPR), arbuscular mycorrhizal fungi and *Rhizobium spp*. in the rhizosphere of *Anthyllis cytisoides*, a model legume for revegetation in mediterranean semi-arid ecosystems. The New Phytologist, 136(4), 667-677.

Revillas, J. J., Rodelas, B., Pozo, C., Martínez-Toledo, M. V., & González-López, J. (2000). Production of B-group vitamins by two *Azotobacter* strains with phenolic compounds as sole carbon source under diazotrophic and adiazotrophic conditions. Journal of applied microbiology, 89(3), 486-493.

Rodionov, D. A. (2007). Comparative genomic reconstruction of transcriptional regulatory networks in bacteria. Chemical reviews, 107(8), 3467-3497.

Rodionov, D. A., Li, X., Rodionova, I. A., Yang, C., Sorci, L., Dervyn, E., ... & Osterman, A. L. (2008a). Transcriptional regulation of NAD metabolism in bacteria: genomic reconstruction of NiaR (YrxA) regulon. Nucleic acids research, 36(6), 2032-2046.

Rodionov, D. A., De Ingeniis, J., Mancini, C., Cimadamore, F., Zhang, H., Osterman, A. L., & Raffaelli, N. (2008b). Transcriptional regulation of NAD metabolism in bacteria: NrtR family of Nudix-related regulators. Nucleic acids research, 36(6), 2047-2059.

Rossolillo, P., Marinoni, I., Galli, E., Colosimo, A., & Albertini, A. M. (2005). YrxA is the transcriptional regulator that represses de novo NAD biosynthesis in *Bacillus subtilis*. Journal of bacteriology, 187(20), 7155-7160.

Rovira, A. D., & Harris, J. R. (1961). Plant root excretions in relation to the rhizosphere effect: V. The exudation of B-group vitamins. Plant and Soil, 199-214.

Rovira, A. D. (1969). Plant root exudates. The botanical review, 35(1), 35-57.9

Scheublin, T. R., Deusch, S., Moreno-Forero, S. K., Müller, J. A., van der Meer, J. R., & Leveau, J. H. (2014). Transcriptional profiling of Gram-positive *Arthrobacter* in the phyllosphere: induction of pollutant degradation genes by natural plant phenolic compounds. Environmental microbiology, 16(7), 2212-2225.

Shaukat-Ahmed, H. J. E. (1961). The essentiality of cobalt for soybean plants grown under symbiotic conditions. Proceedings of the National Academy of Sciences of the United States of America, 47(1), 24.

Sheibani-Tezerji, R., Rattei, T., Sessitsch, A., Trognitz, F., & Mitter, B. (2015). Transcriptome profiling of the endophyte *Burkholderia phytofirmans* PsJN indicates sensing of the plant environment and drought stress. MBio, 6(5), e00621-15.

Sheldrick, G. M. (2015). Crystal structure refinement with SHELXL. Acta Crystallographica Section C: Structural Chemistry, 71(1), 3-8.

Sivasakthi, S., Usharani, G., & Saranraj, P. (2014). Biocontrol potentiality of plant growth promoting bacteria (PGPR)-*Pseudomonas fluorescens* and *Bacillus subtilis*: a review. African journal of agricultural research, 9(16), 1265-1277.

Smith, A. G., Croft, M. T., Moulin, M., & Webb, M. E. (2007). Plants need their vitamins too. Current opinion in plant biology, 10(3), 266-275.

Solano, B. R., Maicas, J. B., & Mañero, F. G. (2008). Physiological and molecular mechanisms of plant growth promoting rhizobacteria (PGPR). Plant-bacteria interactions: strategies and techniques to promote plant growth. Wiley, Weinheim, Germany, 41-52.

Sorci, L., Kurnasov, O., Rodionov, D. A., & Osterman, A. L. (2010). Genomics and Enzymology of NAD Biosynthesis. Comprehensive Natural Products II Chemistry and Biology.

Streit, W. R., Joseph, C. M., & Phillips, D. A. (1996). Biotin and other water-soluble vitamins are key growth factors for alfalfa root colonization by *Rhizobium meliloti* 1021. Molecular plant-microbe interactions: MPMI, 9(5), 330-338.

Verma, J. P., Yadav, J., Tiwari, K. N., & Kumar, A. (2013). Effect of indigenous *Mesorhizobium spp.* and plant growth promoting rhizobacteria on yields and nutrients uptake of chickpea (*Cicer arietinum* L.) under sustainable agriculture. Ecological Engineering, 51, 282-286.

Waller, G. R., Yang, K. S., Gholson, R. K., Hadwiger, L. A., & Chaykin, S. (1966). The pyridine nucleotide cycle and its role in the biosynthesis of ricinine by *Ricinus communis* L. Journal of Biological Chemistry, 241(19), 4411-4418.

Walpola, B. C., & Arunakumara, K. K. I. U. (2016). Assessment of phosphate solubilization and indole acetic acid production in plant growth promoting bacteria isolated from green house soils of Gonju-Gun, South Korea. Tropical Agricultural Research and Extension, 18(1).

Wang, K., Conn, K., & Lazarovits, G. (2006). Involvement of quinolinate phosphoribosyl transferase in promotion of potato growth by a *Burkholderia* strain. Appl. Environ. Microbiol., 72(1), 760-768.

Weekes, D., Miller, M. D., Krishna, S. S., McMullan, D., McPhillips, T. M., Acosta, C., ... & Jaroszewski, L. (2007). Crystal structure of a transcription regulator (TM1602) from *Thermotoga maritima* at 2.3 Å resolution. Proteins: Structure, Function, and Bioinformatics, 67(1), 247-252.

Weilharter, A., Mitter, B., Shin, M. V., Chain, P. S., Nowak, J., & Sessitsch, A. (2011). Complete genome sequence of the plant growth-promoting endophyte *Burkholderia phytofirmans* strain PsJN.

Zakharova, E. A., Iosipenko, A. D., & Ignatov, V. V. (2000). Effect of water-soluble vitamins on the production of indole-3-acetic acid by *Azospirillum brasilense*. Microbiological research, 155(3), 209-214.

Zhang, X., & Mou, Z. (2009). Extracellular pyridine nucleotides induce PR gene expression and disease resistance in *Arabidopsis*. The Plant Journal, 57(2), 302-312

Zhao, Y. (2010). Auxin biosynthesis and its role in plant development. Annual review of plant biology, 61, 49-64.